

AERO INDIA- 2019

The Runway to a Billion Opportunities



Detailed Project Report



DRUTA

The Rapid Eagle



BITS Pilani
Pilani Campus

team garuda



BITS Pilani
Pilani Campus

In Response to Aero India 2019
Application of Aerospace Technologies for the Betterment of the Billion lives (AABB)

January 20, 2019

Team: GARUDA

Undergraduate Student Team
Birla Institute of Technology & Science, Pilani
Pilani Campus

Acknowledgement Number: E-1

To Aero India 2019:

The members of the Team GARUDA, the Undergraduate Student Design Team of BITS PILANI, Pilani Campus hereby grant Aero India full permission to distribute the enclosed *Executive Summary, Final Proposal and Poster* for exhibition at Student Pavilion at Aero India as they see fit.

Thank you,

Team GARUDA,
Undergraduate Design Team
BIRLA INSTITUTE OF TECHNOLOGY AND SCIENCE, PILANI
Pilani Campus,
Vidya Vihar, Pilani,
Rajasthan, India-333031



BITS Pilani

Pilani Campus

In Response to Aero India 2019
Application of Aerospace Technologies for the Betterment of the Billion lives (AABB)

January 20, 2019

Team: GARUDA

Undergraduate Student Team
Birla Institute of Technology & Science, Pilani
Pilani Campus

Acknowledgement Number: E-1

Kunal

Divya

KUNAL GAJANAN NANDANWAR-Team Leader

Undergraduate Student (Mechanical)
Mail: f2015430@pilani.bits-pilani.ac.in
Contact: +91-9001-365-333

DIVYA RATHORE

Undergraduate Student (Mechanical)
f2015758@pilani.bits-pilani.ac.in

Satyam Bhaskar

Animesh Jain

SATYAM BHASKAR

Undergraduate Student (Mechanical)
Mail: f2015420@pilani.bits-pilani.ac.in

ANIMESH JAIN

Undergraduate Student (Mechanical)
f2015694@pilani.bits-pilani.ac.in

Mandalwar

M.S. DASGUPTA

Professor-in-charge
Mechanical Engineering Department
Mail: dasgupta@pilani.bits-pilani.ac.in, msdasgupta@gmail.com

Acknowledgements

Team GARUDA, the Undergraduate Student Design Team of BITS PILANI, Pilani wishes to acknowledge the following people for their invaluable discussion, guidance, and support throughout the course of this project.

BITS PILANI, Pilani Campus Faculty

- *Dr. MS Dasgupta* - Professor and Head of Department, Mechanical Engineering Department BITS Pilani, Pilani
- *Dr. Hari Om Bansal* - Associate Professor, Electrical and Electronics Engineering Department, BITS Pilani, Pilani
- *Dr. Jitendra S. Rathore* - Assistant Professor Mechanical Engineering Department, BITS Pilani, Pilani
- *Dr. Shyam Sundar Yadav* - Assistant Professor Mechanical Engineering Department, BITS Pilani, Pilani

BITS PILANI, Pilani Campus Students

- *Mr. Devashish Bonde* - Bachelor of Engineering, Mechanical Engineering Department (2015-2019)
- *Mr. Rishav Utkarsh* - Master of Science, Physics Department and Bachelor of Engineering, Mechanical Engineering Department (2015-2020)

Contents

Acknowledgements	1
List of Tables	4
List of Figures	6
Introduction	7
1 Vehicle Configuration and Selection	1
1.1 Mission Analysis	1
1.2 Candidate Configurations	2
1.3 Design Criteria	2
1.4 Configuration Ranking	3
2 Initial Vehicle Sizing	4
2.1 Description of the Sizing Algorithm	4
2.2 Vehicle Sizing Considerations	6
3 Tilt Rotor Sizing	9
3.1 Trade Studies	9
3.1.1 Selection of Hover Disk loading	9
3.1.2 Solidity	10
3.1.3 Selection of Blade Aspect Ratio	10
3.1.4 Selection of the Number of Blades	11
3.1.5 Comparison between 5+3 and 4+4 Rotor System	12
3.1.6 Selection of Hover Tip Speed	14
3.1.7 Airfoil Selection	14
3.1.8 Hinge Offset	16
3.1.9 Inter-rotor Spacing	16
3.2 Rotor Design	16
3.2.1 Design Goals	16
4 Rotor Blade Structure and Hub Design	18
4.1 Rotor Blade Structural Design	18
4.1.1 Torque Tube	18
4.1.2 Outer Blade Segment	18
4.2 Hub Design	19
5 Wing and Tail Geometry	21
5.1 Wing Geometry	21
5.1.1 Airfoil Selection	21
5.1.2 Other Wing Parameters	21
5.1.3 High Lift Generating Devices	22
5.1.4 Control Surfaces	22
5.2 Tail Geometry	22

6 Wing Design and Reconfiguration Details	24
6.1 Wing Configuration Selection	24
6.1.1 Considered Configurations	24
6.1.2 Selection Method: Weighted Matrix	25
6.2 Structural Design	26
6.2.1 Retracting Torque Box	26
6.2.2 Retracting Mechanism	27
6.2.3 Initial Sizing	28
6.2.4 Inflation Mechanism	28
6.2.5 Material Selection	28
6.3 Reconfiguration Details	29
7 Drive Train	32
7.1 Engine Selection	32
7.2 Transmission Design	33
7.2.1 System Configuration	33
7.2.2 Gearbox Casing	34
8 Performance Analysis	35
8.1 Drag Estimation	35
8.2 Vehicle Download	35
8.3 Hover Performance	35
8.4 Dash Speed	36
8.5 Range	37
8.6 Autorotational Capability	38
9 Landing Gears	39
9.1 Landing Gear Types Considered	39
9.2 Static Stability Angle Analysis	39
10 Airframe Structure	40
10.1 Structural Details	40
10.2 Material Selection	40
11 Weight and CG Analysis	41
12 Avionics and Control systems	42
12.1 Requirements	42
12.1.1 Avionics and Sensors	42
12.2 Sensor Operation	44
12.2.1 Control system initialization	44
12.2.2 Vertical Flight and Hover	44
12.3 Flight Control System	44
12.3.1 Yaw control	45
12.3.2 Pitch and roll control	46
13 Cost Analysis	47
13.1 Acquisition Cost	47
14 Summary	48

List of Tables

1	Overview of <i>Druta</i>	8
1.1	Design Requirements	1
1.2	Priority Matrix of Design Criteria using AHP	3
1.3	Comparison of candidate configurations using AHP	3
2.1	Approximate Thrust and Power Requirements in Hover and Forward Flight	6
2.2	Actual Thrust and Power Requirement	6
3.1	Rotor blade parameters	15
3.2	Final blade configuration at design point	17
3.3	Efficiency results at design point	17
5.1	Values of the empennage	23
6.1	Weighted decision matrix showing the various configurations ranked against the weighted criteria.	26
6.2	Comparison of Various materials considered for Torque Box	28
6.3	Comparison of properties of various engineering materials for wing skin	29
7.1	Comparison of various engine configurations considered	32
7.2	Selected properties of Rolls Royce M-250 C10B	32
7.3	Properties of the turbojet TJ23U by PBS (Each Engine)	33
7.4	Transmission gear specifications	33
8.1	Cruise speed for different operational altitudes	35
8.2	Hover time values for 50% and 100% fuel usage	36
8.3	Maximum speed values at different operational altitudes	36
8.4	Equivalent drag area for different operational altitudes	37
8.5	Maximum range values for different operational altitudes	37
11.1	Weight and CG Analysis details of <i>Druta</i>	41
12.1	Avionics system components	44
13.1	H factor vs Aircraft properties	47



List of Figures

1	<i>Druta</i> in hover configuration	7
2.1	Generalized mission profile	4
2.2	Flowchart for the vehicle sizing procedure	5
3.1	Variation of Disc loading with diameter	9
3.2	Variation of Blade loading coefficient with Aspect Ratio and Number of Blades	10
3.3	Variation of thrust produced with the Aspect Ratio of rotor blade	11
3.4	Variation of power required with the aspect ratio of rotor blade	11
3.5	Variation of Maximum Gross Take-off Weight with the average number of blades per rotor	11
3.6	Variation of Centrifugal Force experience by each rotor blade with the average number of blades per rotor.	11
3.7	Variation of Power requirement with number of blades	12
3.8	Variation of thrust with tip speed	13
3.9	Variation of power required with thrust produced	13
3.10	Comparative acoustic study between 4+4 and 5+3 coaxial rotor systems	14
3.11	Variation of blade loading coefficient with tip speed	14
3.12	Variation of Power requirement with Tip Speed	15
3.13	Constraints on Choice of Tip Speeds	15
3.14	Variation of C_l and C_l/C_d with angle of attack for NACA 0012 at R.N. 1,000,000 and n_{crit} value 9	16
3.15	Variation of propulsion efficiency with airspeed	17
4.1	Rotor blade in extended configuration (Hover Mode)	18
5.1	C_l vs Angle of attack	21
5.2	C_l vs C_d	21
5.3	V-tail span dimensions	23
6.1	Basic Tensairity beam element	25
6.2	Relative Importance(%) of Wing Configuration Selection Criterion	26
6.3	Retracting Torque Box in Expanded and retracted shape along with ribs and without skin.	27
6.4	Sectional View describing the Retracting mechanism inside Torque box	27
6.5	Low Temperature Properties of Vectran TM Fiber	29
6.6	Reconfiguration procedure	30
7.1	Planetary Gearbox with clutch plate and brakes	34
7.2	Gearbox casing	34
8.1	Variation of hover time with the amount of fuel used	36
8.2	Variation of power required with velocity	37
8.3	Variation of thrust required with velocity	37
8.4	Comparison of autorotative index for different rotorcraft	38
9.1	Gearbox casing	39



LIST OF FIGURES

12.1 General flow diagram of signal flow	42
12.2 Avionics components	43
12.3 Roll, Pitch and Yaw control in hover configuration	45
12.4 Roll, Pitch and Yaw control during cruise	45
12.5 Design of Control systems for <i>Druta</i>	46
14.1 <i>Druta</i> in both hover and forward flight configuration over a mega city	48



Introduction

The helicopter's high degrees of maneuverability and hover capabilities are undeniably important performance features in today's domestic and international security environment. While able to hover for hours depending on fuel levels, conventional helicopters are limited by the rotors aerodynamics to a limited top speed. On the other hand, fixed-wing planes can reach much faster speeds, but are unable to hover with a great degree of efficiency. The challenge is to merge the aerodynamics required for hover capabilities and the propulsion necessary to achieve greater speeds 'without unacceptable compromises in range, efficiency, useful payload or simplicity of design'. The proposed *Druta* contra rotating tiltrotor design with spanwise adaptive wings attempts to provide the forward flight speed equivalent to fixed wing planes within the same size and weight constraints. The biggest challenge for the team was to reduce the weight along with increasing the range and maximum forward flight speed and to keep the maximum span of less than 3 m length.

The design methodology of *Druta* is focused on (1) Reducing the gross takeoff weight (2) Reducing the power requirement in hover especially (3) Maximizing the forward flight speed (4) Maximizing the cruise range.



Figure 1: *Druta* in hover configuration

Table 1: Overview of *Druta*

Mission Requirement & Design Solution	Section number
Max Gross Takeoff Weight of 600 kg	Use of composite materials and Inflating wings maintains an empty weight fraction of 0.61.
333 km/h or greater max airspeed	Innovative combination of main turboshaft engine and two small turbojets help <i>Druta</i> reach a maximum airspeed of 535 km/h
Maximum vehicle span of less than 3 m in hover	A coaxial rotor system with 5 and 3 blades and spanwise adaptive wings make <i>Druta</i> an efficient and compact design.
Maximize hover time in hours	Hover optimized design gives a hover time of 74 minutes with 50% fuel capacity. It is through use of coaxial rotor system with 5 and 3 blades which provides low disk loading and retracted wings which decrease down wash area.
Maximize cruise efficiency	Variable diameter rotor and using only main turboshaft engine in cruise maximize the cruise efficiency. Range of <i>Druta</i> at a cruise velocity of 61.8 m/s is 498 km at 3000 m altitude.
Reduced drag area	Maximizing the area for wings and optimized aerodynamics reduces the drag area to 0.11 sq m at 3000m altitude.
Reliable control	<i>Druta</i> uses swashplate in hover configuration while aileron and inverted V-tail in forward flight configuration for quick and reliable control.
Autonomous reconfiguration	Avionics allow for a fully autonomous flight and reconfiguration by components which remain onboard the aircraft at all times.

1. Vehicle Configuration and Selection

A detailed analysis of V/STOL wheel[1] was done. Various configurations were analyzed on the basis of design requirements for a megacity type environment. This section discusses the tradeoff study involved in the final configuration selection.

1.1 Mission Analysis

In order to understand the requirements of the design, a careful study of the given RFP was done. Three civilian oriented missions were developed to further understand the mission segments and performance characteristics during each phase of the mission. Table 1.1 shows the proposed design requirements on the basis of developed missions.

Table 1.1: Design Requirements

Maximum Gross Takeoff Weight	600 kg
Maximum Vehicle Footprint Size (in hover)	3x3 m
Minimum Payload Capacity	100 kg
Required Maximum Airspeed in Forward Flight	333 km/h or 92.5 m/s
Service ceiling height	3000m

The virtual missions created to benchmark the system are:

- **Surveillance inside a city:** The system would start the mission from an operational base or launch point outside the city roughly 300 km away and attain cruise flight while approaching the city. Then it would switch over to hover mode roughly 2km away from the city limits. It would then enter the city in loiter stance and perform the required surveillance operation. With the necessary payload onboard, the system will be able to either detect chemical agents in the atmosphere or test for trace radioactive signatures. The system is also equipped with an on-board camera to use when required. After the mission objective is satisfied, it will return to base by first exiting the city limits and only then transitioning to forward flight.
- **Supply drop inside a city:** The system would perform the same operation as stated above until entering the city in a hover stance. Then it will land at a predesignated spot and drop off its cargo. In situations without a suitable landing spot (like a flooded area) the system can hover close to the ground and accurately drop the cargo. This kind of a mission is suited for disaster relief management. The system can reach from a relatively far away base in short time and land precisely at a given spot. Hence, it is better than a standard parachute air-dropped disaster relief package which would not be able to reach a precise location. Furthermore, it can land at multiple locations to drop-off multiple packages with relative ease.
- **Rural operations:** The system has been designed for urban operations, but it is also usable in an open area. Like any standard drone, it can be deployed from a base to reach a location over which it can either loiter for surveillance or land to deliver cargo and return to base.

1.2 Candidate Configurations

To maximize the hover time of *Druta* at sea-level standard altitude (SLS) and at 3000 m standard atmosphere, two main factors were considered:

- Efficiency with respect to power required for given thrust
- Minimizing the drag due to downwash of the rotor blade system

The design drivers considered can be achieved with a limited number of configurations only. A thorough comparative analysis was carried out using well known vehicle configurations and several new concepts. The following candidate configuration were listed for detailed analysis and comparison.

- **Single main rotor:** Due to a constraint on maximum vehicle footprint during hover configuration, a single main rotor will require greater number of rotor blades to provide the required thrust. It makes the design very complex and reduces the efficiency. Single main rotor also requires tail rotor to balance the angular momentum . Tail rotor adds weight and does not contribute to lift.
- **Ducted rotor:** Ducts increase the thrust by a considerable amount but use of ducts would rule out the swashplate based control and would require use of vanes or other devices for primary control. The other ways to control includes the use of bleed, compressed air or vanes but they increase the complexity and weight.
- **Tip Jets:** Jets are placed on the tips of rotor blades but if the size of rotor is small then exhaust of one jet interferes with others inlet causing inefficiency. Also smaller jets have a higher SFC. Also reliability of tip jets is very low as failure of a single jet can lead to crash.
- **Tandem/ Intermeshing/ transverse/ multirotor:** These configurations leave a large amount of area as useless, increasing the disc loading and hence the power requirement. To have the most efficient hovering, optimum use of area provided should be there. These would typically have higher empty weight due to requirement of powering two equal rotors. This sacrifices compactness and results in smaller rotors with higher disc loading and therefore, lower hover efficiency.
- **Deflected slipstream:** The basic principle is to deflect the slipstream from one or more propellers approximately 90 degrees, to create an upward thrust for vertical takeoff and a downward air cushion for landing. Once airborne, the flaps are retracted so the airplane can fly horizontally. This deflection of slipstream leads to a wastage of energy. Also, it leads to very unstable configuration in Hover.
- **Coaxial:** Coaxial configuration saves weight as all the power is used in generating lift, no tail rotor is required and single transmission and hub is required for both the rotors. Both rotors can utilize the maximum length span condition thereby decreasing the power requirement in Hover. The inherent compactness of the configuration (lack of tail rotor) can allow for larger individual rotors with low disc loadings and high hover efficiency which can overcome the losses due to the aerodynamic interference between the two rotors.

1.3 Design Criteria

The major design criteria identified based on mission requirements are :

- **Hovering Efficiency:** Hovering efficiency represented in the form of power loading (thrust/power) is most critical design parameter towards efficient design of rotor.
- **Empty Weight Fraction:** Given the weight of payload, lower empty fraction would imply less power consumption .

CHAPTER 1. VEHICLE CONFIGURATION AND SELECTION

- **Power Loss Due to Anti-Torque (AT) System:** The anti-torque system consumes a significant amount of the available power. Therefore, the anti-torque generation mechanism with least power loss would be the most desirable.
- **Compactness:** Less than 3m span in Hover configuration makes compactness a very important design criteria.
- **Low Speed Manoeuvrability:** It would ensure that the vehicle can maintain its position during hover with accuracy.
- **Technical Maturity:** Use of unproven technology in the design decreases the reliability. Technical Maturity however restricts the innovation in the design.
- **Cruise Efficiency:** Cruise at higher L/D ratio will lead to higher endurance. It is desirable feature for every flight vehicle.

1.4 Configuration Ranking

To evaluate the different concepts and determine which configuration best satisfied the requirements of the missions, the team went through a comprehensive analysis in which an Analytical Hierarchy Process (AHP) matrix[2] is generated.

Table 1.2: Priority Matrix of Design Criteria using AHP

Priority Configurations Matrix	Hovering Effi-cency	Empty Wt. Frac-tion	Power Loss to AT System	Compactness	Low Speed Maneuverabil-ity	Technical Matu-rity	Cruise Effi-ciciency	Total
Hovering Efficiency	1	2	2	3	4	4	3	0.28
Empty Wt. Fraction	0.5	1	0.5	0.5	3	3	2	0.15
Power Loss to AT System	0.5	2	1	1	2	2	3	0.17
Compactness	0.33	2	1	1	3	3	2	0.18
Low Speed Maneuverability	0.25	0.33	0.5	0.33	1	0.5	0.75	0.05
Technical Maturity	0.25	0.33	0.5	0.33	2	1	0.5	0.07
Cruise Efficiency	0.33	0.5	0.33	0.5	1.5	2	1	0.09

Table 1.3: Comparison of candidate configurations using AHP

Priority Configurations Matrix	Hovering Effi-cency	Empty Wt. Frac-tion	Power Loss to AT System	Compactness	Low Speed Maneuverabil-ity	Technical Matu-rity	Cruise Effi-ciciency	Total
Weightage	0.28	0.15	0.17	0.18	0.05	0.07	0.09	
Single Main Rotor	0.7	0.5	0.2	0.3	0.6	0.5	0.3	0.45
Ducted Rotor	0.8	0.3	0.2	0.2	0.6	0.5	0.2	0.42
Tip jets	0.6	0.5	0.2	0.3	0.5	0.2	0.3	0.40
Tandem	0.6	0.2	0.7	0.1	0.6	0.5	0.4	0.44
Deflected slipstream	0.2	0.3	0.7	0.2	0.3	0.3	0.5	0.34
Coaxial	0.7	0.5	0.7	0.5	0.5	0.4	0.4	0.57

AHP results shows that Coaxial is the most suitable configuration according to the mission requirements. The second most suitable configuration is single main rotor but due to constraint of less than 3 m span, using single main rotor will lead to exceptionally high values of disc loading. Therefore without any further selection procedure, coaxial configuration was selected.

2. Initial Vehicle Sizing

Two missions are considered during the sizing of *Druta*. The first mission requires the aircraft to achieve high speed forward flight (relative to current VTOL aircraft). Secondly it require efficient hover through the use of novel reconfigurable propulsive and lifting devices. The aircraft has to be designed in taking consideration that it has to be operated in the Megacity-type-environment for the surveillance purposes. Considering the requirements of both the missions, *Druta* is designed to be capable of high forward flight speeds, good hover efficiency and with a good acoustic signature. Because a tiltrotor is a hybrid of a fixed-wing aircraft and a helicopter, a new method was developed for sizing the aircraft. This method included changes to the estimation of the mission weights and weight fractions, which incorporates the empty takeoff weight, payload, the power requirements and the fuel weight. This new sizing method was conducted for each of the missions specified above.

2.1 Description of the Sizing Algorithm

Tishchenko's method is constituted of basic methodologies and algorithms centered around historic data that have been extensively validated for determining the size and weight of a helicopter. While this methodology is fairly general in its applicability to most rotorcraft concepts, several modifications were necessary to provide the flexibility needed to design tiltrotor configurations[3]. The missions outlined were first decomposed into mission segments, as shown in Figure 2.1, and the sizing method was used to compute the power requirements and fuel quantity required to complete each segment of the defined mission. It was also necessary to account for the change in relevant equations for the power required in forward flight when in full airplane mode.

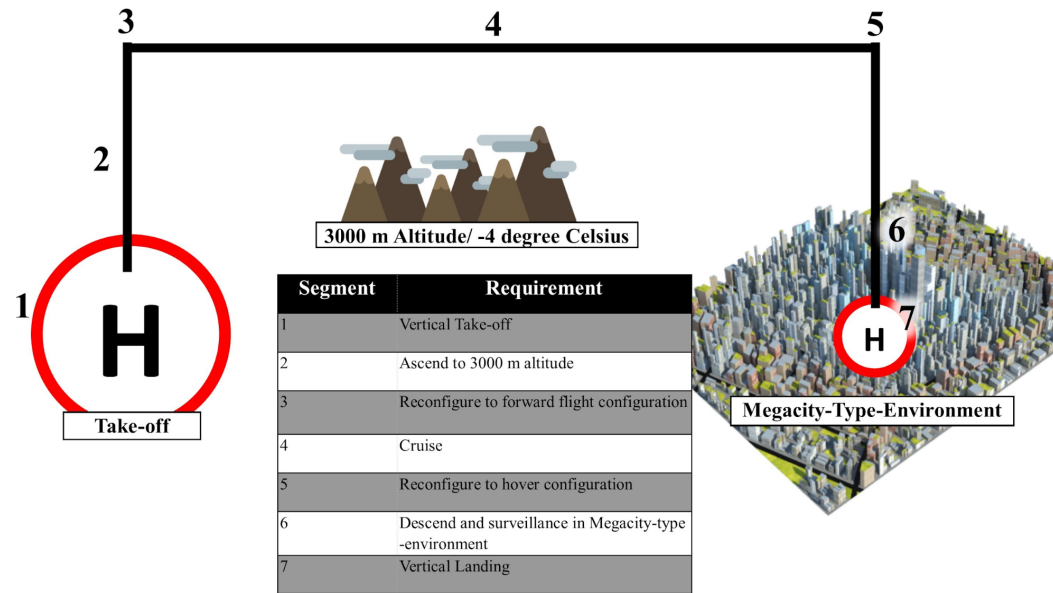


Figure 2.1: Generalized mission profile

CHAPTER 2. INITIAL VEHICLE SIZING

The component weight equations in Tishchenko's method were replaced with the equations used in NASA Design and Analysis of Rotorcraft (NDARC) methodology[4]. The NDARC equations account for, amongst other things, wing related items that are sized based, in part, on the structural stiffness requirements needed for propeller-based aircraft.

A schematic of the design algorithm is shown in Figure 2.2. The process is iterative and begins with the specification of particular mission requirements, including the desired range, payload, and cruise speeds, as well as the operational altitudes and atmospheric conditions. Estimated initial values of rotor figure of merit, propulsive efficiency, transmission efficiency, engine installation losses, aspect ratios of the wing and blades, rotor disk loading, hover tip speeds, and number of blades are also required. These parameters are, however, changed during the design iterations to obtain the vehicle with the best efficiency in hover and forward flight.

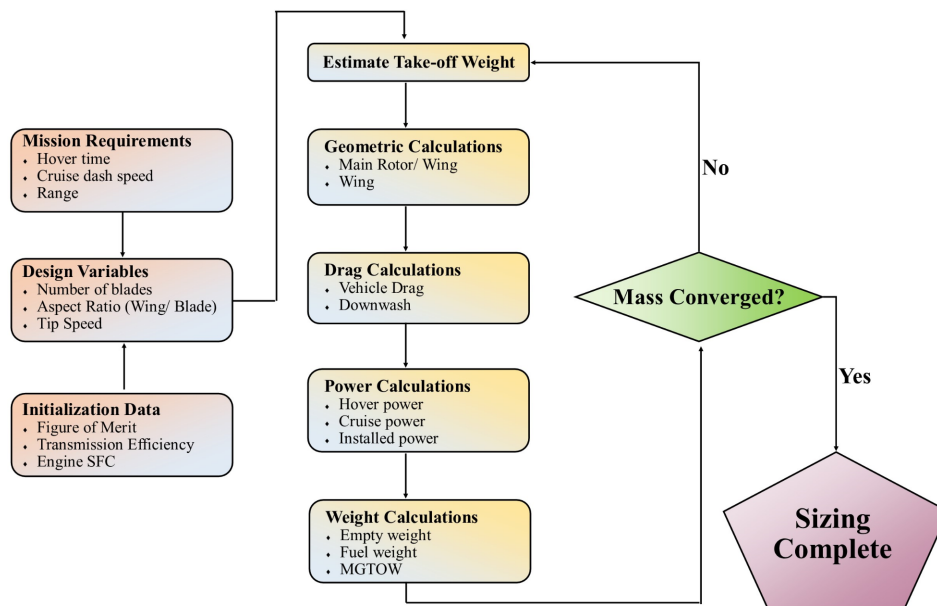


Figure 2.2: Flowchart for the vehicle sizing procedure

The steps in the sizing procedure are carried out as follows:

- Mission requirements are specified and initial vehicle characteristics are provided.
- An initial estimate is made for the MGTOW of the vehicle to be designed based upon historical data.
- From the disk loading desired in hover, the rotor diameter is calculated.
- With the user defined blade aspect ratio and the rotor diameter, the blade chord is computed.
- The power required in hover is based on the MGTOW, disk loading, figure of merit, and the vertical download on the vehicle in hover.
- The wing span is calculated based on geometric constraints, which include the rotor diameter, an estimate for the fuselage width, and the necessary spacing between the rotors and the fuselage for reasons of operational safety. With the aspect ratio of the wing defined, the wing chord is also determined.
- The estimated parasitic drag area, in conjunction with the wing dimensions, are used to calculate the cruise power requirements. Because of the relatively high cruise altitude re-

CHAPTER 2. INITIAL VEHICLE SIZING

quirement (altitude of 3000 m), the cruise power also determines the installed power available at mean sea level (MSL) ISA conditions.

- Based on the power requirements in each segment of the mission, the total mass of fuel required is calculated.
- The empty weight equations are used to estimate the total empty weight.
- The MGTOW obtained at the end of each iteration is used as a starting point for the next iteration.

The above procedure is repeated until convergence is obtained, based on the relative error between the initial and final value of the MGTOW. This procedure was carried with regards to the mission to determine the sizing of the vehicle.

2.2 Vehicle Sizing Considerations

Before trade studies were conducted to determine the optimal set of blade parameters, an analysis was conducted to determine the most demanding mission. With respect to the power requirement, preliminary calculations showed the need to be much greater for hover than for forward flight. The table 2.1 shows the variation of the approximate values of thrust requirement and power requirement for the hover and cruise configuration.

Table 2.1: Approximate Thrust and Power Requirements in Hover and Forward Flight

	Thrust Requirement (N)	Power Requirement (kW)
Hover	6000	170
Forward Flight	350	50

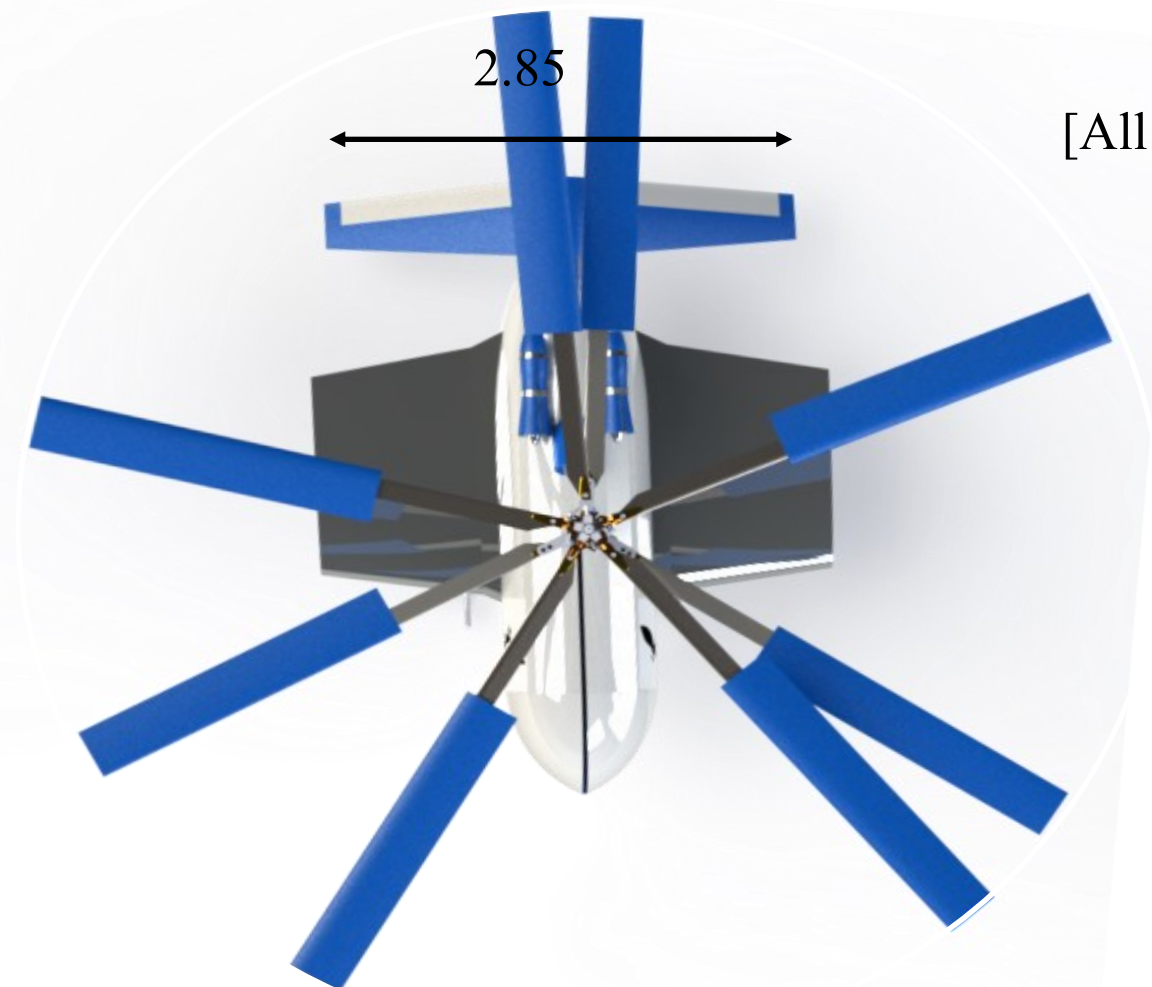
The following methodology was adopted to determine the vehicle sizing:

- Hover configuration was selected as the potential sizing configuration.
- Parameters such as the vehicle weight, diameter of the rotor and size/capacity of the fuel tanks were determined.
- The “sized” aircraft was used to perform the forward flight. The rpm, power and efficiency are calculated to get the desired thrust.
- Rotor diameter is changed to meet proper efficiency and tip speeds in the permissible range to achieve the thrust requirement.
- The sizing mission was obtained by repeating the above steps such that the required thrust is obtained with the minimum power requirement.

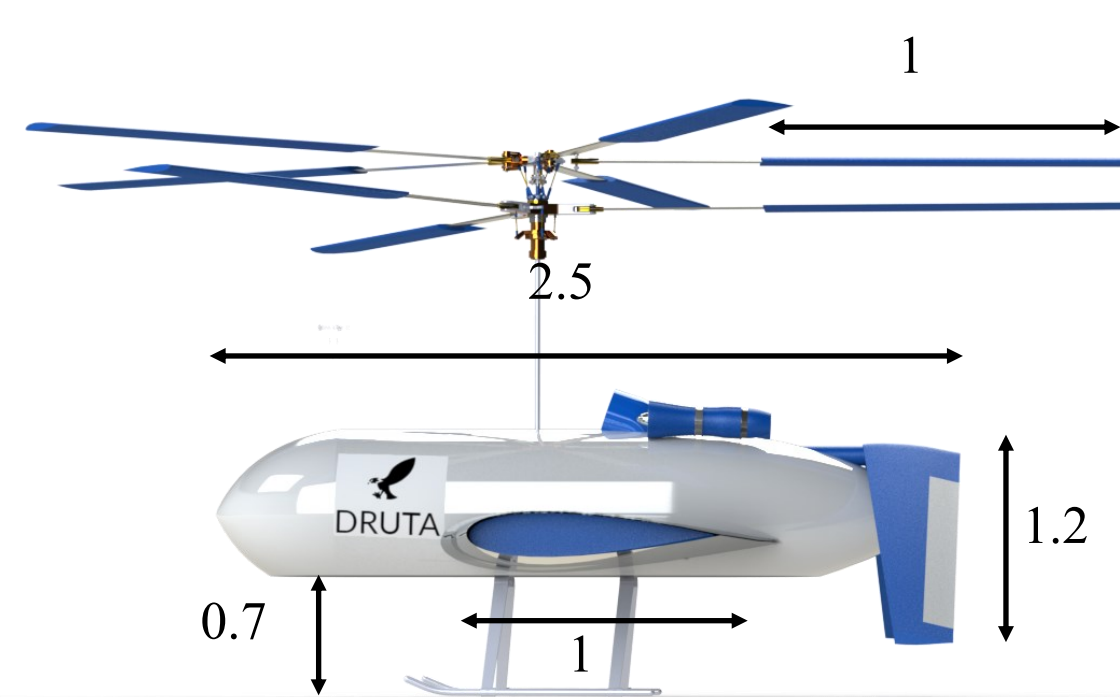
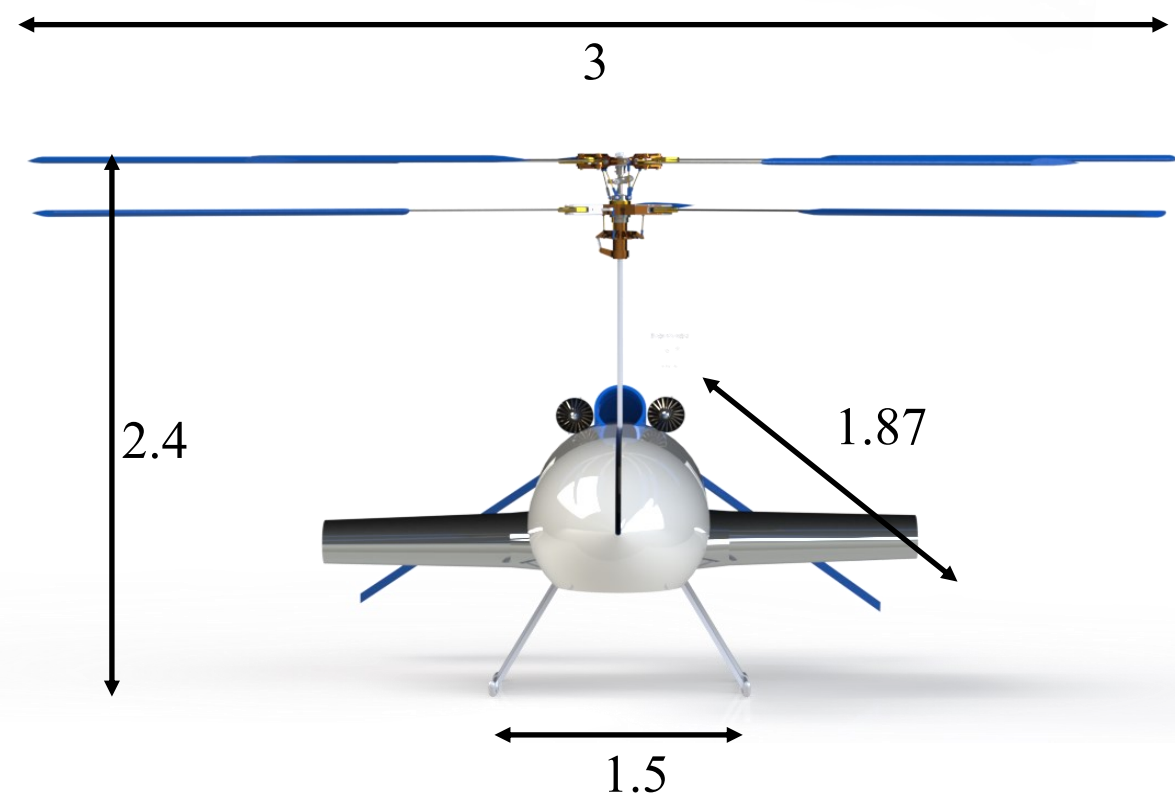
Table 2.2: Actual Thrust and Power Requirement

	Thrust Requirement (N)	Power Requirement (W)
Hover	6240	167741
Forward Flight	355	29177

Hover Four View



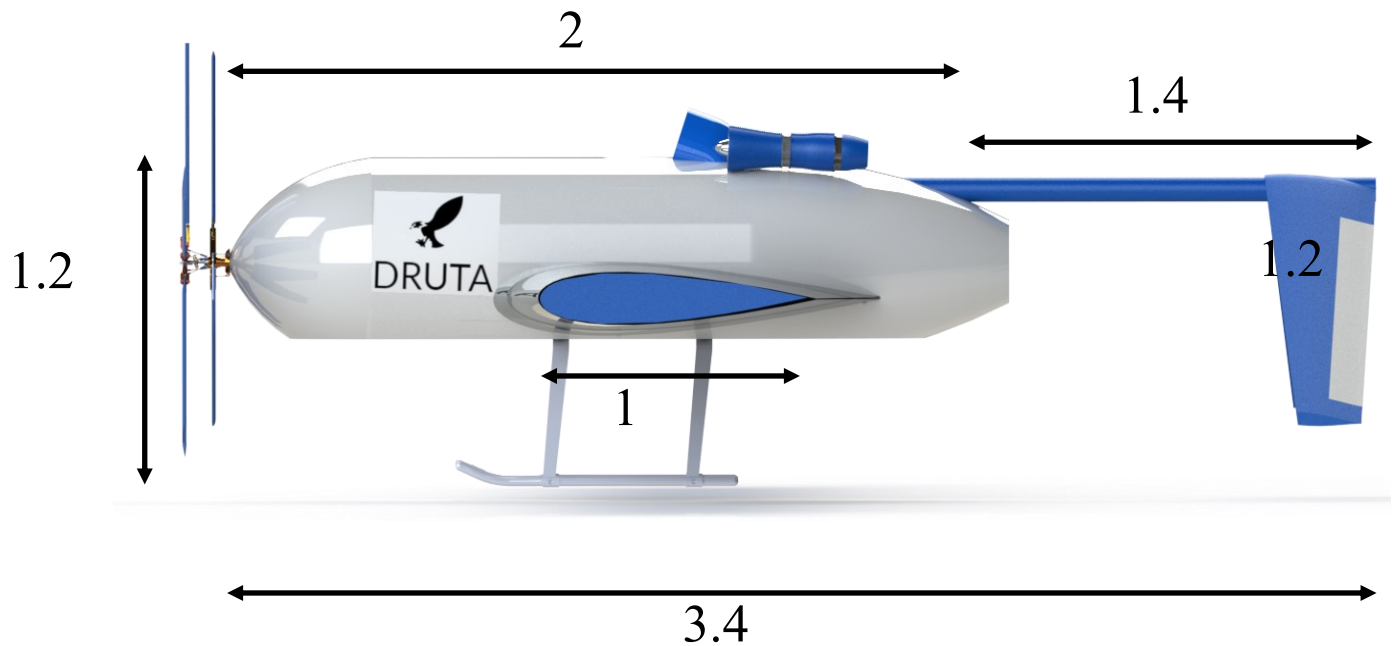
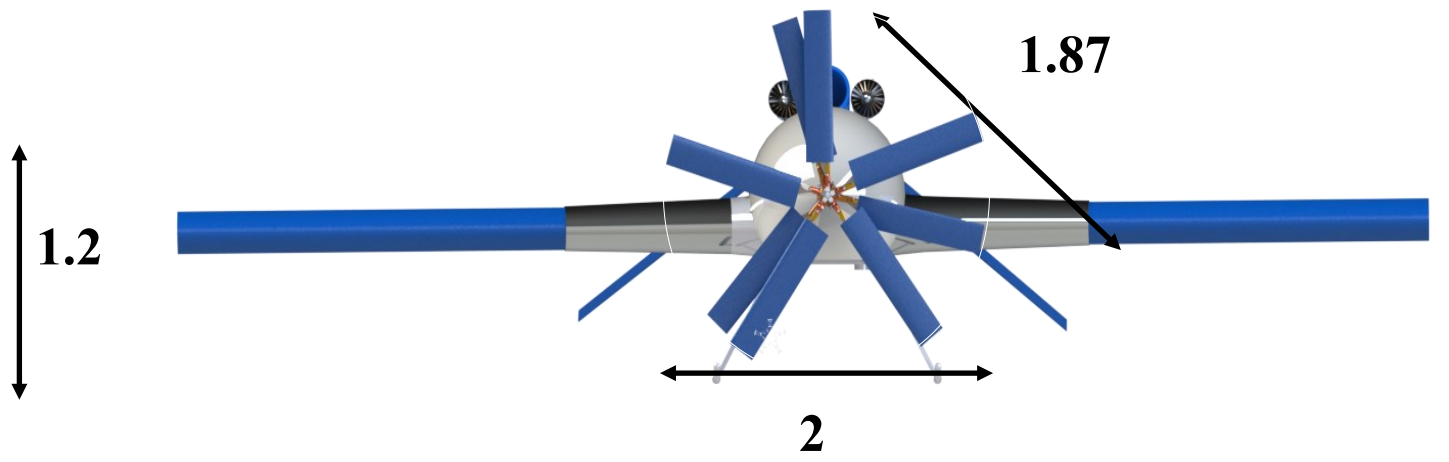
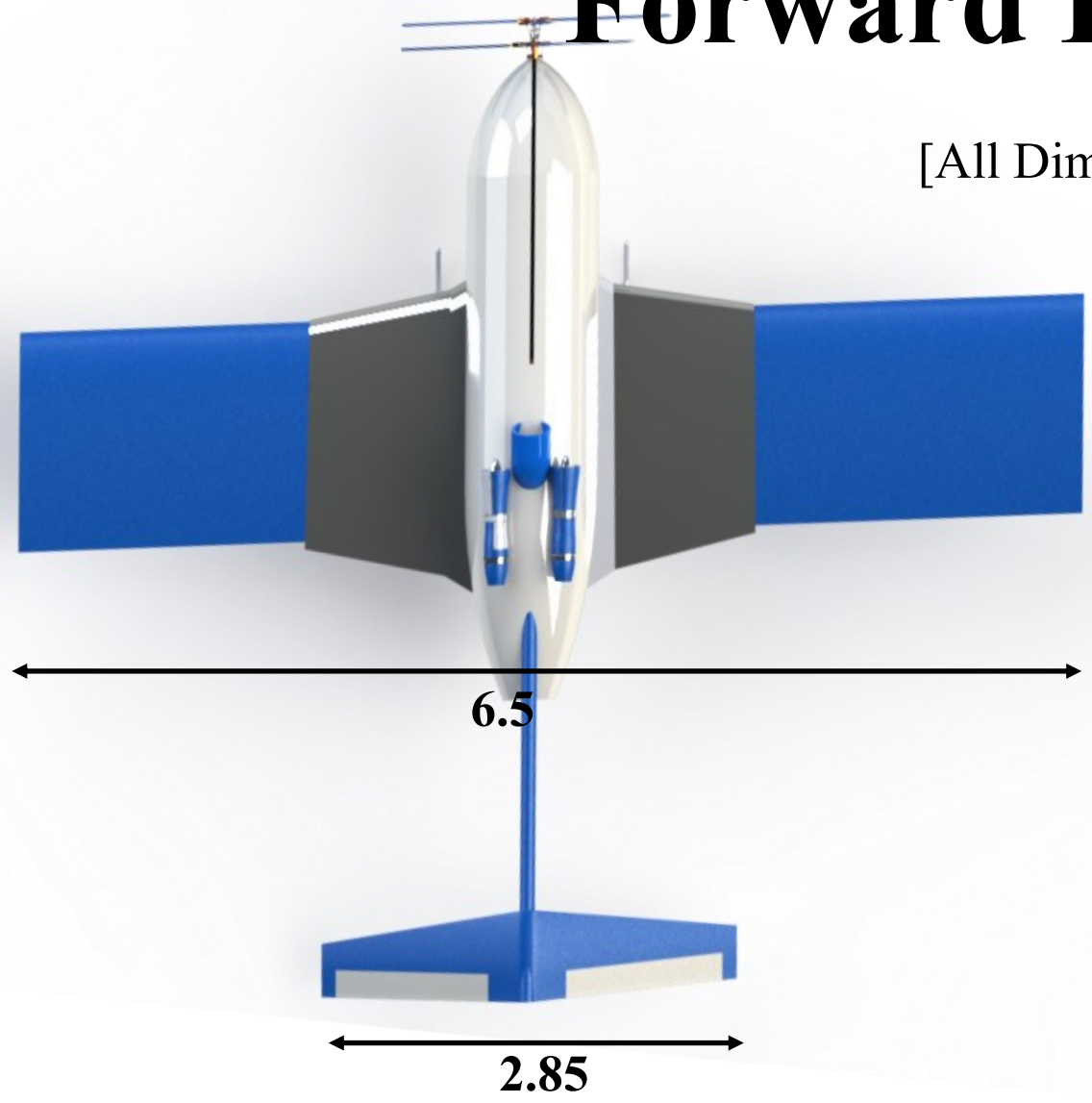
[All Dimensions in meter (m)]



Forward Flight Four View



[All Dimensions in meter (m)]



3. Tilt Rotor Sizing

3.1 Trade Studies

3.1.1 Selection of Hover Disk loading

While operating in a Megacity-type-environment, high downwash velocities can make the operating environment below the vehicle challenging and hazardous. Traditional tiltrotor concepts have relatively high disk loadings, typically varying from 88–117 kg/m², because the rotor is sized more to maximize propulsive efficiency. Hence, for a good hovering efficiency and safe near-ground flight operations, a tiltrotor ideally requires a low disk loading, if this can be obtained without significantly compromising the propulsive efficiency. Figure 3.1 shows the variation of rotor diameter against disc loading for the same conditions mentioned previously. The higher the loading, the more power needed to maintain rotor speed[5]. A low disc loading is a direct indicator of high lift thrust efficiency[6].

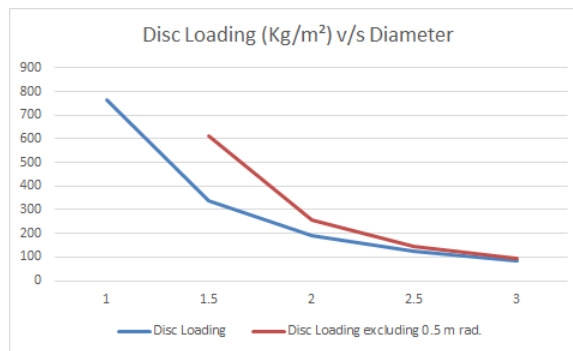


Figure 3.1: Variation of Disc loading with diameter

Increasing the weight of a helicopter increases disk loading. For a given weight, a helicopter with shorter rotors will have higher disk loading, and will require more engine power to hover. A low disk loading improves autorotation performance in rotorcraft.

Lower disk loading will increase efficiency, so it is generally desirable to have larger propellers from an efficiency standpoint. Maximum efficiency is reduced as disk loading is increased due to the rotating slipstream; using contra-rotating propellers can alleviate this problem allowing high maximum efficiency even at relatively high disc loadings.

The benefits of a large rotor, however, must be weighed against forward flight efficiency and the various other practical aspects of designing a vehicle with large rotors. There are some problems with smaller disk loadings which leads to larger blades as mentioned below:

- Longer blades are more prone to vibration and resonance dynamics, if for no reason other than that their rigidity is reduced by length, holding all else constant.
- Longer blades provide less operating clearance.
- Longer blades not only stall before shorter blades (retreating), but also hit the critical Mach number at lower air speeds(advancing).

Since forward flight is not a major concern in this reconfigurable VTOL, in the helicopter configuration, also being it unmanned and having very less allowable limit of 3 m, these problems

would not affect the flight. However, to get a good propulsive efficiency, diameter has to be decreased in the forward flight configuration. A root radius of 0.5 m has been chosen to be excluded in the hover configuration so that it could be retracted back during cruise. Taking all this into consideration, a disk loading of 95 kg/m^2 at MGTOW of 600 kg was selected. This does not vary much from typical tilt rotors and is the minimum possible disk loading in the allowable limit. Using contra-rotating propellers further increases the maximum efficiency as compared to conventional rotors.

3.1.2 Solidity

The solidity was chosen in conjunction with the hover tip speed to give the necessary stall margin. The factors affecting solidity selection are the number of blades and the blade aspect ratio. Figure 3.2 shows the effect of aspect ratio and number of blades on the blade loading coefficient. Increasing the number of blades from three to four can increase the available stall margin.

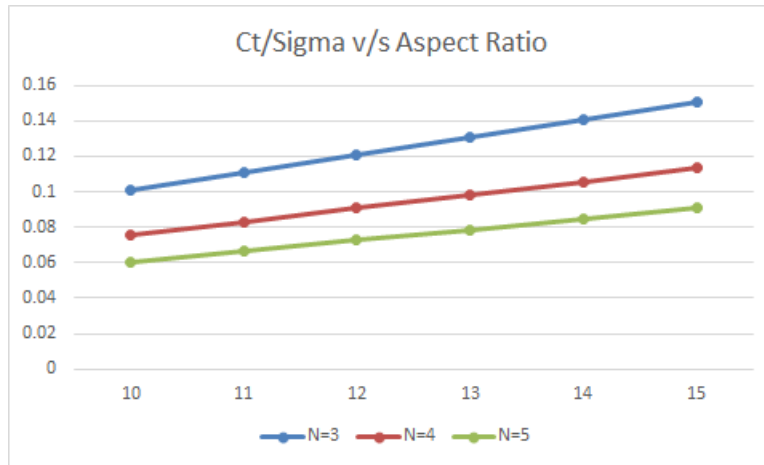
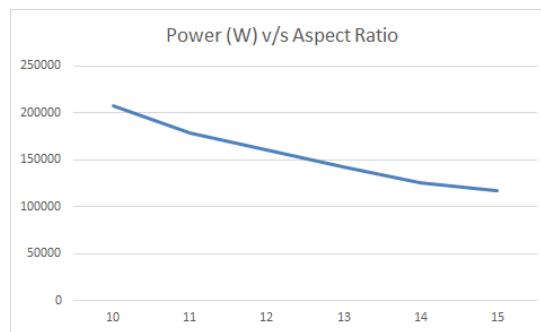
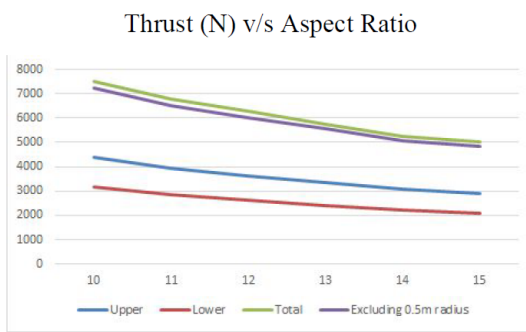


Figure 3.2: Variation of Blade loading coefficient with Aspect Ratio and Number of Blades

3.1.3 Selection of Blade Aspect Ratio

The blade aspect ratio is related to the solidity of the rotor system. A higher blade aspect ratio will result in a lower solidity when the number of blades are held constant, which will result in a lower blade loading coefficient, and, as a byproduct, a rotor with lower vibrations and reduced noise. However, selecting a large aspect ratio defines a blade with a long radius that can limit propulsive efficiency in cruising flight. A lower aspect ratio blade for a given disk loading, tip speed, and thrust coefficient (CT), will result in a higher blade loading coefficient (CT/σ , where σ is the rotor solidity). However, decreasing solidity is undesirable because the corresponding increase in CT/σ reduces the stall margin of the rotor, which must always be retained for maneuverability and gust response, and especially because of the requirement to operate at 3,000 m, -4.49 Celsius. Figures 3.3 and 3.4 show that an increased aspect ratio is beneficial in reducing the vehicle MGTOW and installed power. Based on considerations set by the disk loading and CT/σ for a fixed tip speed and number of blades, a blade aspect ratio of 11.8 was selected.

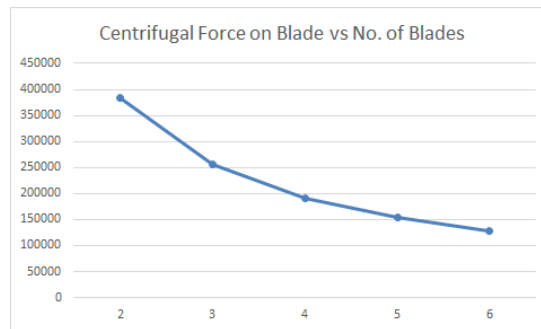
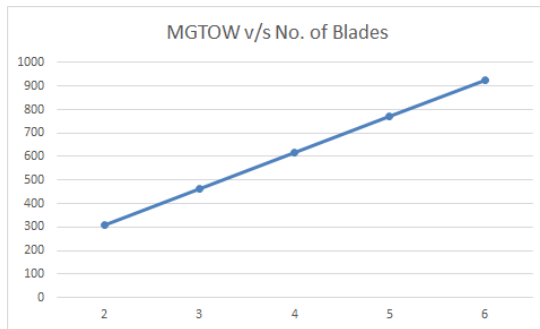


3.1.4 Selection of the Number of Blades

The number of blades used on the rotor affect the centrifugal force experienced by each blade as centrifugal force decreases with an increase in the number of blades, however, with a higher number of blades the hub would become more complex and heavier. With blade aspect ratio, tip speed and rotor disc area being fixed, a minimum of 4 blades per rotor system is required to achieve the lift.

A lower centrifugal force even helps in the retraction of the blades. The increase in vehicle MGTOW versus the number of blades shown in Figure 3.5 is shown.

$$No. \text{ of } Blades = (No. \text{ of } blades \text{ in upper rotor} + No. \text{ of } blades \text{ in lower rotor})/2 \quad (3.1)$$



The centrifugal force on each blade decreases between a 3- and 5-bladed rotor design, as shown in Figure 3.6.

Initial trade studies showed that increasing the number of blades increased the takeoff power requirements, as shown in Figure 3.7.

For a constant CT, a superior stall margin is achieved by increasing the solidity of the rotor. This dictates either increasing the number of blades or decreasing blade aspect ratio. Therefore, for a fixed aspect ratio, disk loading, and tip speed, the effect of increasing number of blades was studied.

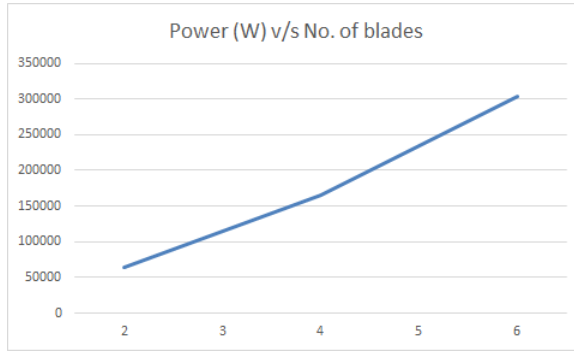


Figure 3.7: Variation of Power requirement with number of blades

For operation in the Megacity-type-environment, the noise produced by the rotor system begin to play an important role for the convenience of the livelihood. It has been observed from the acoustic study that the main factor responsible for the unbearable sound production in coaxial configuration is the beats production due to overlapping of the upper and lower rotor at a definite interval of time while in motion. To overcome this, a novel idea of using a 5+3 rotor system has been proposed, so as to disrupt the perfect gap in time interval within rotor overlap and causing non uniform cross over thus interrupting resonance.

3.1.5 Comparison between 5+3 and 4+4 Rotor System

A comparison between 5+3 rotor system and 4+4 rotor is performed on the basis of thrust produced with the change in tip speed keeping all other specifications constant, and the power required with the variation of thrust produced. Also the acoustic studies is performed to determine the beat formation and the noise production.

Thrust Requirement

Varying the tip speed, the thrust produced is observed. It should be noted that the thrust produced with 5+3 rotor system is much greater than 4+4 rotor system, keeping the solidity constant. 4+4 rotor system could not even achieve the required thrust of 6000+ N with the maximum permissible tip speed of 240 m/s, with an aspect ratio of 11.8. 20% more thrust is produced compared to conventional coax-system at constant tip speed of 232m/s.

Power Requirement

The power required is calculated for both the configurations and the variation with the thrust produced has been observed. The power required for the 5+3 system is lesser than that of 4+4 system for the same amount of thrust production. As the lower blade is considered to be always in vertical flight configuration, and the power required increases with the gain in speed, determined by the following formula:

$$\Delta P = T \left[\frac{V_c}{2} + \sqrt{\frac{V_c^2}{2} + v_{1_h ov}^2 - v_{1_h ov}} \right] \quad (3.2)$$

The thrust produced by the lower rotor is much less than that of upper rotor, ratio being 0.72:1, to produce same amount of torque in opposite direction. The lower amount of thrust results in the requirement of lesser power, giving better efficiency and more hover time to *Druta*.

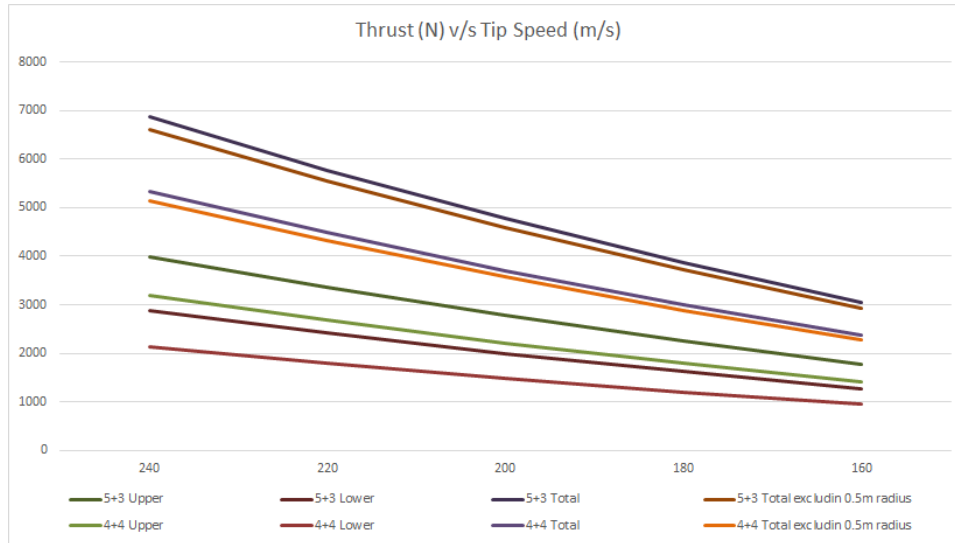


Figure 3.8: Variation of thrust with tip speed

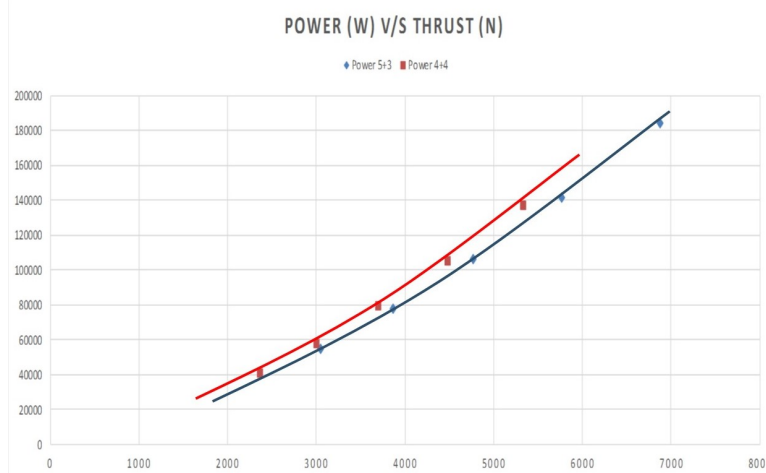


Figure 3.9: Variation of power required with thrust produced

Acoustic Studies

A comparative acoustic study between the two types of rotor system has been done. Coaxial rotors increases the amount of noise as compared to conventional rotors. The main reason behind the noise of coaxial rotors is the formation of beats due to the regular overlap of rotors[7]. To reduce this, an idea of having non symmetrical rotor systems is proposed.

In the 4+4 rotor system, there is a definite interval of 0.0065 seconds (angular velocity = 155 rad-s) when all the 4 rotors overlap simultaneously. Where as in 5+3 rotor system, only 1 rotor overlap at a time with a relatively lesser interval of time of 0.0014 seconds, causing much higher frequency. As well as the relative noise produced with 5+3 configuration is 25% that of conventional coaxial rotor system of 4+4 rotors.

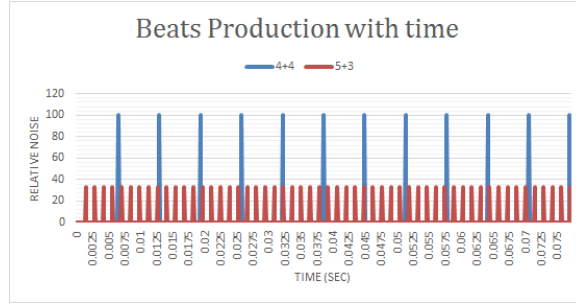


Figure 3.10: Comparative acoustic study between 4+4 and 5+3 coaxial rotor systems

3.1.6 Selection of Hover Tip Speed

A higher tip speed in hover is beneficial in lowering the blade loading coefficient (CT/σ) providing a higher stall margin for maneuvering. Additionally, higher tip speeds benefit the design by providing good auto rotational performance, thus increasing the kinetic energy stored in the rotor system. However, for the same level of thrust, increasing tip speed will adversely affect the profile power and rotor noise. A higher tip speed results in higher profile power losses leading to a lower power loading. This latter effect is reflected in the increase in installed power for increasing hover tip speed, as shown in Fig. 3.12. A higher tip speed also increases rotor noise. *Druta* can afford to operate at relatively high tip speeds in hover because the Variable Diameter Rotor concept lowers the tip speed in forward flight, thereby maintaining cruise efficiency. Considerations of flow compressibility also play an important role in the selection of hover tip speed.

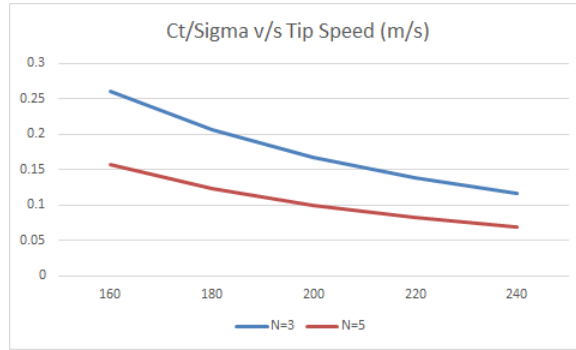


Figure 3.11: Variation of blade loading coefficient with tip speed

3.1.7 Airfoil Selection

The physical dimensions of *Druta* vehicle and operating conditions results in the airfoil operating largely in the low Mach number and low Reynolds number regimes. The desirable characteristics for such an airfoil are:

- High $c_{l_{max}}$ that is insensitive to Reynolds number
- Gentle stall characteristics
- Airfoil camber of less than 5% to prevent excessive moment about the aerodynamic center
- Thickness-to-chord greater than 10% to provide the necessary structural strength

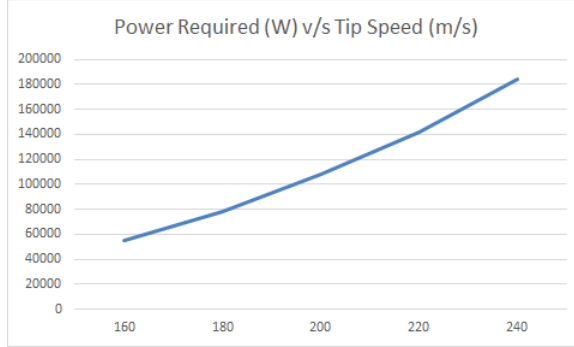


Figure 3.12: Variation of Power requirement with Tip Speed

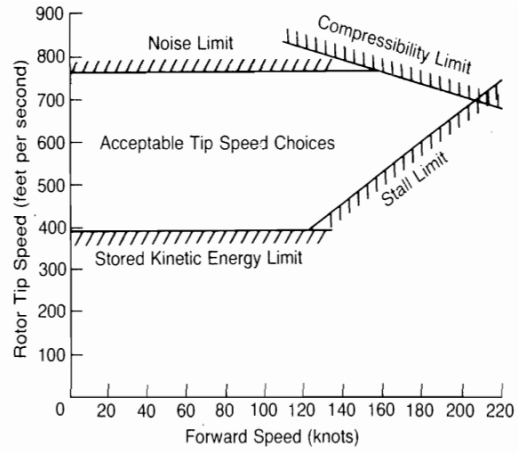


Figure 3.13: Constraints on Choice of Tip Speeds

The preliminary study used a NACA0012 airfoil baseline blade[8]. This airfoil has been well studied and is a natural choice for helicopter blades so the chosen airfoil for *Druta* is the NACA0012. This airfoil has a thickness of 12% at 30% chord, and a 0% camber, $c_{l_{max}} = 1.39$ and a maximum lift-to-drag ratio of 75.6.

The rotors of *Druta* are designed for efficient hover performance at sea level conditions. The rotor diameter, number of blades, chord length, aspect ratio, tip speed and required thrust coefficient were estimated for the best performance. Both the rotors are contra-rotating, rotating at same angular velocity with upper rotor rotating in clockwise (CW) direction and lower rotor in counter clockwise (CCW) direction.

Table 3.1: Rotor blade parameters

	Upper Rotor	Lower Rotor
Aspect Ratio	11.8	11.8
Number of Blades	5	3
Blade Chord	0.127 m	0.127 m
Tip Speed	235 m/s	235 m/s

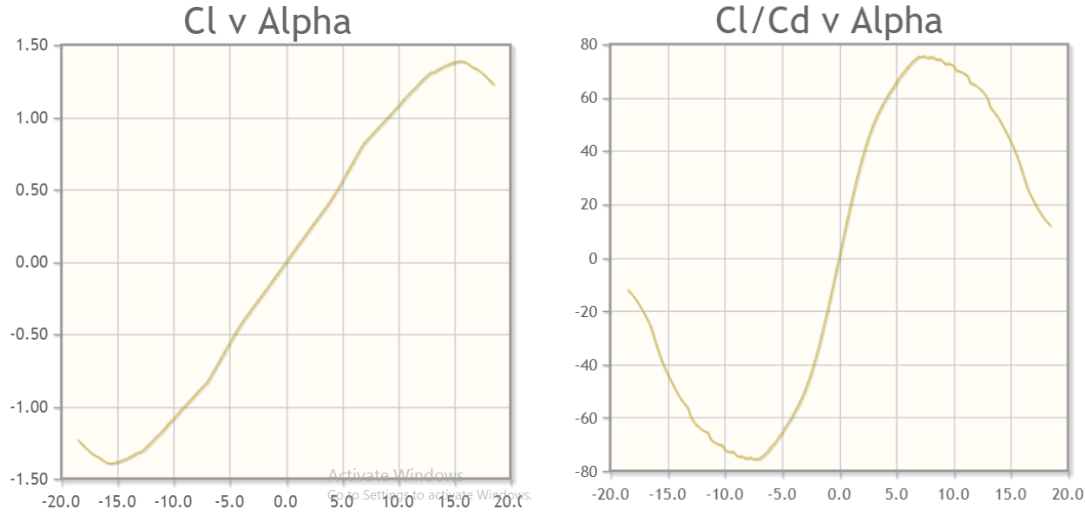


Figure 3.14: Variation of Cl and Cl/Cd with angle of attack for NACA 0012 at R.N. 1,000,000 and $ncrit$ value 9

3.1.8 Hinge Offset

Higher hinge offset increases the control moment of the helicopter. However, the manoeuvrability requirements from the current design are not very critical. Hence, *Druta* is given a moderate hinge offset of 0.10R for low vibrations and small hub drag by providing a virtual hinge through material tailoring.

3.1.9 Inter-rotor Spacing

In coaxial helicopters, there is a need to ensure adequate clearance between the upper and lower rotors to avoid the physical contact between the two rotor blades due to the flapping motion. The rotor spacing also influences the performance of the helicopter which is in itself a major field of research. For *Druta*, rotor spacing (h/D) was chosen to be 0.09, i.e 0.27m.

3.2 Rotor Design

Druta presents a unique set of aerodynamic and structural design challenges. Aerodynamically, an optimal combination of parameters, such as blade twist and rotor solidity, must provide desired performance in hover and forward flight, despite the dissimilar design drivers between these flight conditions. Beyond the aerodynamic challenges, *Druta* must also perform the extension/retraction while maintaining a high level of reliability, structural efficiency, and dynamic stability over the operational range of RPMs. This section presents the systematic aerodynamic methodology and structural design of *Druta*.

3.2.1 Design Goals

One of the key challenges associated with tiltrotor design is the need for the rotor to operate efficiently both in helicopter and airplane flight modes, respectively. The figure of merit, described as FM in Eq. 3.3, was computed during development of the rotor as one measure of the hovering

CHAPTER 3. TILT ROTOR SIZING

efficiency. The propulsive efficiency, denoted as ηP in Eq. 3.4, was also computed to help evaluate the forward flight efficiency[9, 10].

$$FM = \frac{P_{Ideal}}{P_{Actual}} = \frac{(C_{T,U} + C_{T,L})^{3/2}}{\sqrt{2}(C_{P,U} + C_{P,L})} \quad (3.3)$$

$$\eta_P = \frac{2}{1 + \frac{V_{final}}{V_{flight}}} \quad (3.4)$$

Modern aircraft have propulsive efficiency ηP in the range of 0.80 to 0.90. A rotor diameter of 3 m could not achieve a good propulsive efficiency and hence needs to be reduced. A retracted diameter of 1 m is chosen to operate in the forward flight configuration. Figure 3.15 shows the variation of propulsion efficiency with aircraft speed. Reduction in rotor diameter increased the propulsion efficiency by 14%.

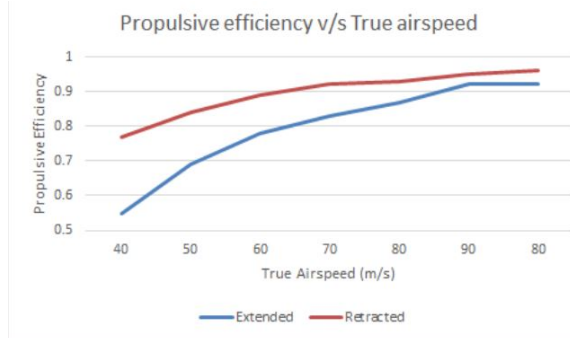


Figure 3.15: Variation of propulsion efficiency with airspeed

An ηP of 0.89 at the design point of 62 m/s at 3,000 m and an FM=0.75 at 3000 m is achieved ensuring the hovering thrust efficiency remained comparable to modern helicopters. These values drove the final design of the rotor, which is summarized in Table 3.2 and Table 3.3.

Table 3.2: Final blade configuration at design point

Twist rate = -4 (degree/m)	Upper Rotor	Lower Rotor
Hover	-6 degree	-6 degree
Cruise	-4 degree	-4 degree

Table 3.3: Efficiency results at design point

Solidity	ηP	FM
0.1080.	0.89	0.75

4. Rotor Blade Structure and Hub Design

4.1 Rotor Blade Structural Design

The rotor blade consists of two primary structural members: an inner, non-lifting elliptical segment (torque tube) and an outer, lifting blade segment. During extension/retraction modes of operation, the outer blade segment telescopes over the inner elliptical section, permitting a change in the overall diameter of the rotor.

Radius of rotor is changed from 1.5 m hover configuration to 1 m in forward flight configuration. To accomplish this change, an antenna type retraction mechanism similar to wing is used. This mechanism is described in detail in section 6.2.2. There are two parts in the antenna, torque tube and outer blade segment.

4.1.1 Torque Tube

The torque tube spans upto 0.5 m. The torque tube has a hollow center for the passage of straps for the extension/retraction mechanism. The center of the torque tube is aligned with the quarter chord of the outer-blade section. Furthermore, the torque tube has a linear twist rate of -4 degree, equivalent to the twist rate of the inboard section of the outer blade segment. The equal twist rates permit the outer blade segment to telescope over the torque tube during retraction/extension.

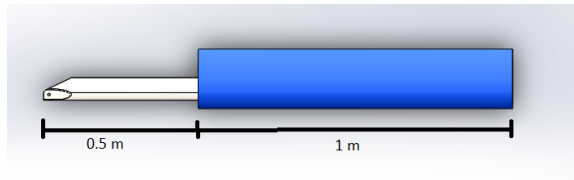


Figure 4.1: Rotor blade in extended configuration (Hover Mode)

The torque tube is constructed of unidirectional fiberglass providing high tensile strength while minimizing material cost. Its high strength and stiffness characteristics allow the blades to be lighter, while their high damage tolerance, superior fatigue properties, and their soft failure modes increase structural integrity and safety. In addition to this, composites offer greater resistance to corrosion, less demanding to repair and have a fatigue-life of up to five times longer than comparable Aluminium alloy blades.

4.1.2 Outer Blade Segment

The outer blade segment spans from 0.5 m to the blade tip. Several blade spar configurations were considered to determine the optimum solution to support the blade structure. D-spar design is chosen as it offers a simple, closed-section structure with high torsional rigidity. The spar extends from a chordwise position of $0.024c$ to $0.4c$ from the leading edge. The D-spar is constructed with layers of unidirectional fiberglass with rohacell foam as the core.

The internal structure of the blade assembly was designed with adequate flap bending , lead-lag bending , torsion bending , and axial stiffness to sustain the centrifugal/compressive buckling loads, steady and oscillatory flap, lead-lag, and torsional moments and shear stresses resulting from aerodynamic and inertial forces.

CHAPTER 4. ROTOR BLADE STRUCTURE AND HUB DESIGN

The outer blade skin consists of carbon fabric and unidirectional fiberglass to provide high bending stiffness and minimize weight. Rohacell foam is selected as the core material. The advantages of this foam is, it has excellent dynamic strength, light weight material and can be easily machined into desired shapes. A tungsten mass ballast weight is used in the nose of the blade to bring the centre of gravity marginally ahead of quarter-chord, which is required to ensure aeroelastic stability of the blades. The trailing edge is made of chopped carbon fibre strands mixed with epoxy. This was done to make the trailing edge rigid and to make it easily machinable. The outer blade skin consists of one layer of unidirectional fiberglass and layers of carbon fabric. Erosion of the rotor blade leading edges due to collision with water, particles, sand and debris is an important consideration. This will reduce the aerodynamic performance as result of flow separation. So, the front half of the blade is covered with sheet made up of steel.

4.2 Hub Design

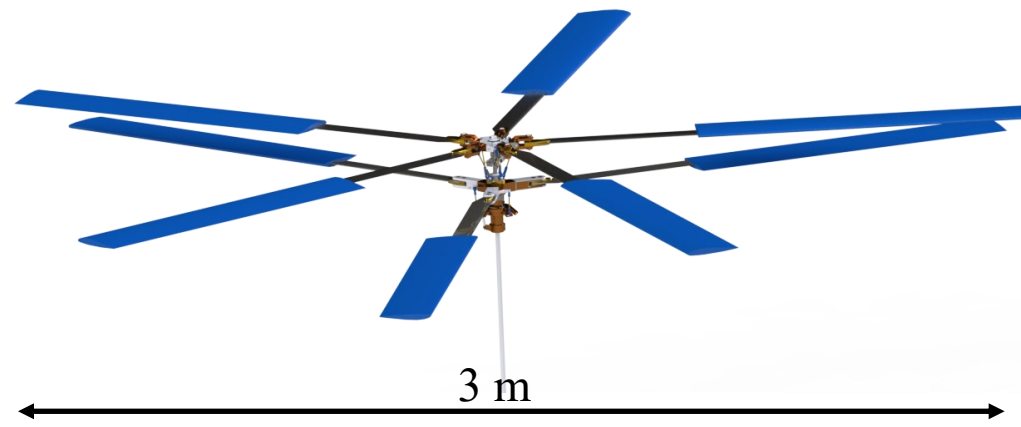
For the design of *Druta*, various rotor hub systems were considered. The constraint of weight demands a rotor hub design that is mechanically simple, while still providing the control authority to respond to wind gusts. Ultimately, these constraints led to the selection of a rigid rotor hub. The following qualitative assessments were used while comparing the different hub configurations.

- **Semirigid Rotor System:** A semirigid rotor system is usually composed of two blades that are rigidly mounted to the main rotor hub. The main rotor hub is free to tilt with respect to the main rotor shaft on what is known as a teetering hinge. This allows the blades to flap together as a unit. Since there is no vertical drag hinge, lead/lag forces are absorbed and mitigated by blade bending.
- **Rigid Rotor System:** The rigid rotor system shown is mechanically simple, but structurally complex because operating loads must be absorbed in bending rather than through hinges. In this system, the blade roots are rigidly attached to the rotor hub. The system is fundamentally easier to design and offers the best properties of both semirigid and fully articulated systems.
- **Fully Articulated Rotor System:** Fully articulated rotor systems allow each blade to lead/lag , flap independent of the other blades, and feather. Fully articulated rotor systems are found on helicopters with more than two main rotor blades.
- **Hingeless:** Hingeless hubs use the flexure to control both flap and lag motion while still using a bearing to control pitch. Because the flap and lag motion are both controlled by the flexure, these hubs often have significant flap-lag coupling and high vibratory Loads.
- **Bearingless:** Bearingless rotors are mechanically simple designs in which all three degrees of motion are controlled by the flexure design of the hub. However, because of redundant load paths, these designs add a significant level of complexity to the structural dynamics design.

To design the hub of *Druta*, we gave priority on mechanical simplicity and reduced maintenance, so a **fully rigid system was chosen**. The rigid rotor system is very responsive and is usually not susceptible to mast bumping like the semi rigid or articulated systems because the rotor hubs are mounted solid to the main rotor mast. This allows the rotor and fuselage to move together as one entity and eliminates much of the oscillation usually present in the other rotor systems. Other advantages of the rigid rotor include a reduction in the weight and drag of the rotor hub and a larger flapping arm, which significantly reduces control inputs. Without the complex hinges, the rigid rotor system becomes much more reliable and easier to maintain than the other rotor configurations[11].

5+3 Retractable Coax Rotor System

EXTENDED

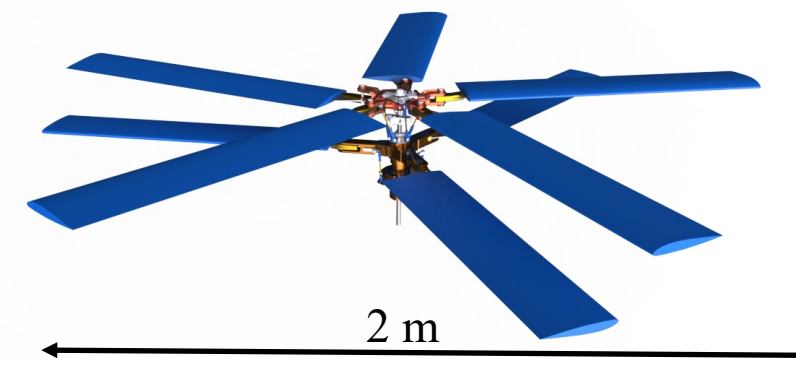


Extended blade
Twist = -6 degree
A.R = 11.8
Chord = 0.127 m

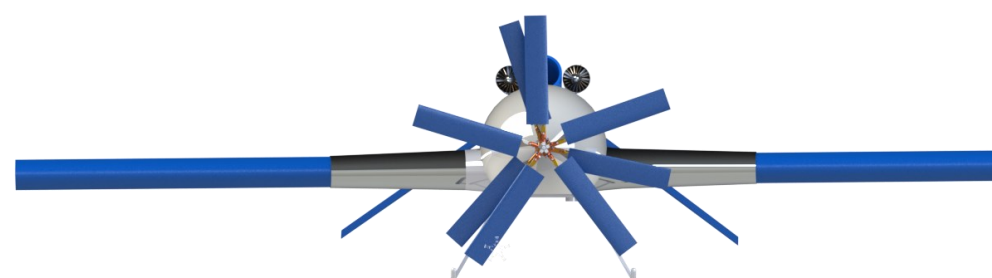


Extended Blade in
Hover
configuration

RETRACTED

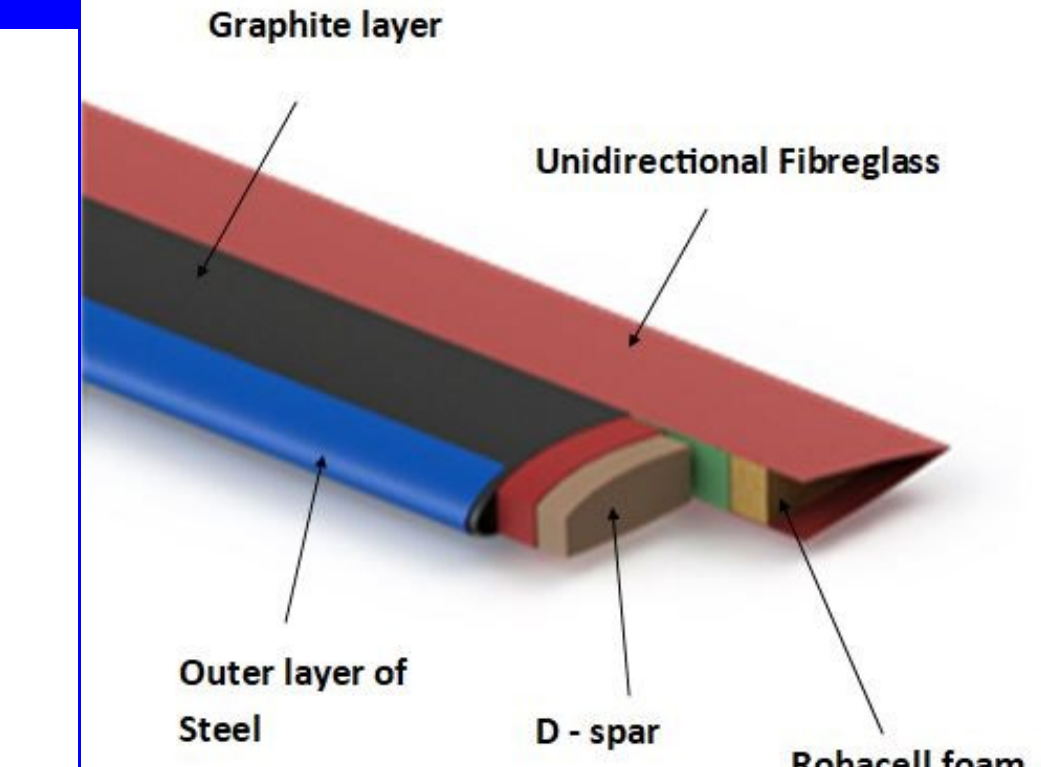


Retracted blade
Twist = -4 degree
A.R = 11.8
Chord = 0.127 m

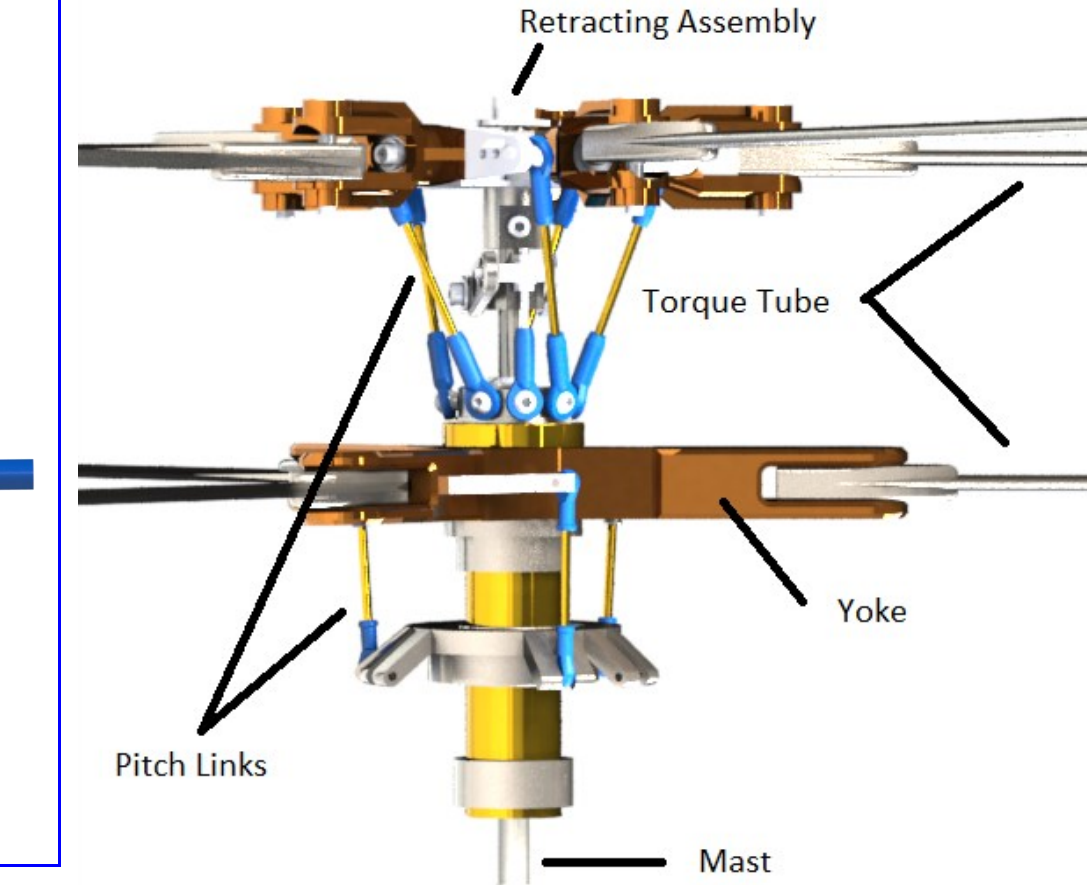


Retracted Blade in forward flight
configuration

CROSS SECTION OF ROTOR BLADE



RIGID ROTOR HUB



5. Wing and Tail Geometry

5.1 Wing Geometry

5.1.1 Airfoil Selection

The basic shape was decided based on the limits of the extending wing structure. The airfoil selection was based on the NACA 5-digit series because the series was originally designed such that the surface roughness has little effect on the airfoil performance parameters[12]. Since cloth is the surface in question, which has a higher surface roughness than the polished metal surface used in traditional airplanes, the use of NACA 5-digit series is justified.

The first digit of the series is based on the design lift coefficient. In the initial phase of the design, a conservative estimate of 0.3 was taken for the coefficient of lift. This served its purpose in finding the required reference area needed for the wing. After testing for different desired steady flight speeds, it was found that the conservative estimate was accurate[13].

The next two digits were chosen by having the maximum camber position at the quarter chord point. This was done so that the structural design of the expandable wings could follow the conservative estimates of the quarter chord point being the aerodynamic center of the wing section.

The last two digits for the thickness to chord ratio were left at the behest of optimizing the structural shape of the torque box. A thickness ratio of 12% was chosen.

The following images show the lift and drag characteristics of the NACA 25112 airfoil. The values are obtained from the *Xfoil prediction tool* at ncrit value of 9 and reynolds number of 1,000,000.

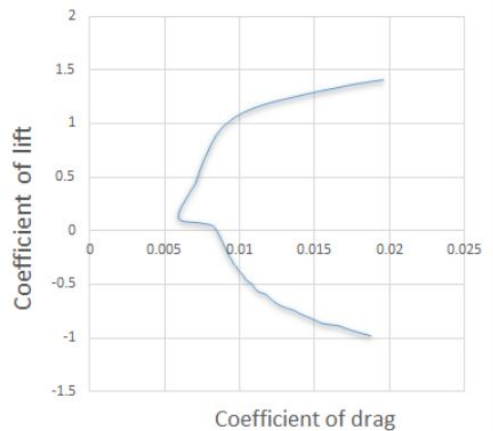


Figure 5.1: C_l vs Angle of attack

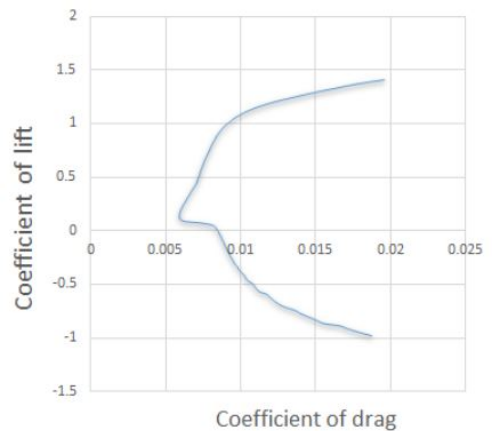


Figure 5.2: C_l vs C_d

5.1.2 Other Wing Parameters

For wing incidence angle, the angle of attack for required coefficient of lift at the cruise speed is chosen. For the chosen NACA airfoil, this angle is 3 degrees.

A classical lower wing dihedral wing was chosen for *Druta*. This ensured stability and lighter

CHAPTER 5. WING AND TAIL GEOMETRY

frame weight. A conservative dihedral of 5 degrees was chosen.

Taper of the wing is generally used to give a closer to elliptical lift distribution along the span, which reduces the induced drag of the wing. Giving a taper would increase the structural complexity of the extendable wing structure. Cloth warping due to the taper would compromise the aileron control surface while in operation. Hence, a wing without taper would be the best compromise between the aerodynamics and structural complexity.

Twist is generally added to a wing to control partial wing stall and the stall region over the span of a wing. In this case, a twist was not added because of the way extending torque box and structural spars operate.

Wing sweep is used to reduce wave drag in high speed forward flight. Since *Druta* does not exceed a forward flight speed of Mach 0.7, there is no requirement for wing sweep. Furthermore, wing sweep tends to reduce the lift generation capacity of a wing at low speeds. Hence, the wing sweep is kept at 0°.

5.1.3 High Lift Generating Devices

High lift devices help a plane generate more lift at the cost of increased drag during low speeds like landing and take-off. In our case, instead of traditional devices, the wings would fully extend during the low speed phase of transition and partially retract once in the cruise speed range. The amount of retraction required was calculated by the net area needed to sustain lift at maximum possible angle of attacks and required speed. The area needed for optimal lift during low speed flight (below 40 m/s) was 7.5 sq. meter with in cruise flight the required lifting area was only 6.5 sq. meter.

The choice of using this method to have two possible wing planform areas has uses in long range missions as well. *Druta* has better glide capabilities with the wing extended to maximum area. Conversely, the cruise speed is lower in this configuration. When it is required to go at a higher speed, the wings can be partially retracted to allow for such high speeds.

5.1.4 Control Surfaces

The ailerons are sized to be contained within 2 ribs of the inflatable wing structure. These ribs hinge about 20% of the chord from the trailing edge to create the control surface area that provides roll control to *Druta*. During the partial extension or retraction of the wing, the innermost ribs get folded into the holding box to ensure the ailerons remain functional during both the wing configuration positions.

The yaw and pitch controls are handled by the combined effect of the ruddervators. The installation of which is done in the V-tail. The tail extends backward with the use of a simple extension beam mechanism. The increased distance of the tail from the C.G of the whole body is essential for the proper pitch control of the system when in forward flight. The ruddervators are explained further in the tail geometry section of the report.

5.2 Tail Geometry

Various tail configurations were considered for the design. V-tails were found to offer the most advantages in the design. According to Raymer[14], V-tails offer reduced interference drag. The V-tail uses ruddervators, a combination of elevators and rudders, whose control is achieved by blending the rudder and elevator control inputs. An inverted V-tail is used to counter the "adverse roll-yaw coupling" effect. Instead, it produces a desirable "proverse roll-yaw coupling" effect. The inverted V-tail also reduces spiraling tendencies.

CHAPTER 5. WING AND TAIL GEOMETRY

The tail is retracted during the hover phase and is kept close to the body so as to fit the 3m x 3m box restriction. In forward flight, the distance of the tail from the main body is found from the tail volume coefficient formula. A horizontal tail volume coefficient of 0.5 and a vertical tail volume coefficient of 0.02 was taken. The values for the V-tail were computed by treating the tail as a pythagorean sum of the horizontal and vertical tails. The angle the V-tail makes with the horizontal is 40 degrees, a near conservative value to ensure the horizontal span of the tail respects the 3m x 3m footprint restriction. The distance between the tail aerodynamic center and C.G of main body was limited by the strength of the extendible rod. No sweep was used in the V-tail. The following table shows the values of the empennage.

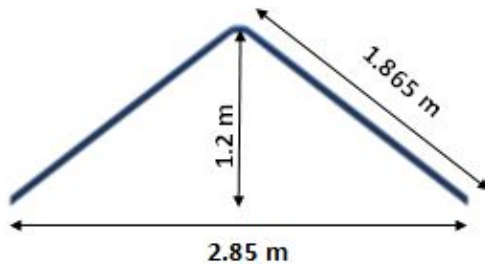


Figure 5.3: V-tail span dimensions

Table 5.1: Values of the empennage.

Tail Section	Vertical Tail	Horizontal Tail	V-tail
Area (sq. m)	0.39	1.625	1.0075
Aspect Ratio	1.5	3	3.45
Taper Ratio	0.8	0.8	0.8
Span (m)	0.765	2.208	1.865
Root Chord	0.566	0.817	0.6
Tip Chord	0.453	0.654	0.48

The control surfaces employed on the V-tail, the ruddervators, are sized such to cover most of the tail area. The span of the control surface is 90% of the tail span. While the chord is 20% of the tail chord.

6. Wing Design and Reconfiguration Details

6.1 Wing Configuration Selection

A novel configuration of spanwise adaptive wings is chosen to reduce the weight of wing group and projected length in hover for *Druta*. Various possible alternatives were considered which include inflating wings, folding and unfolding truss wings, variable sweep wings, retracting torque box design and tensairity structures wings. A decision matrix was used to choose the final wing design.

6.1.1 Considered Configurations

Inflatable Wings

An inflatable wing is designed such that constant internal wing pressure is required to maintain wing shape. High stiffness is achieved with low inflation pressure by maximizing inflated sectional moment of inertia. Since the wing is constructed of a flexible fabric material, it can be stowed by folding or rolling. The outer wing (restraint) and internal baffles are constructed from high strength fibers such as Kevlar. The skeleton of the wing was made of inflatable tubes, surrounded with crushable foam to provide the airfoil cross-section.

To maintain suitable wing strength and stiffness in five-foot span inflatable wing, nitrogen gas pressurization of about 1380-1725 kPa (200-250 psi) was required[15].

Flexibility of Inflatable gives them the capability to recover from gusts and crashes. Also it gives an opportunity to actively morph the wing for control. However due to this flexibility either high pressure, thick wings, low aspect ratio or a combination of these factors is necessary to get enough stiffness for a certain load capability. Since wing stiffness is a function of inflation pressure, and thus aero-elastic behavior is a concern. It also means that any leak, however small, will result in the rapid depressurization of the wing and loss of structural integrity.

Folding Wings

Folding and unfolding wing structure design consists of primary and secondary wing structure in which secondary or extendable structure is connected to primary through a hinged juncture. Of the many retractable wings known to the art, none have been found to be practical enough for adaptation. The main reason for this being in the structural weaknesses that existed at the junctures of the main wing or body and the secondary wing. To overcome the weaknesses materials can be strengthened with braces but the additional braces and structure are complex or heavy.

Major issues with folding and unfolding wings are to provide a retractable airplane wing which is rigid, sturdy and yet light in weight. Another major challenge is to provide a means which would engage or lock the main wing and the secondary wing together such that it forms a substantially rigid structure without having abrupt ends, irregular surfaces or protrusions which would interfere with the normal air stream encountered at high speeds.

Moreover, the ability to fold wings in flight is dependent on heavy and bulky conventional motors and hydraulic systems, which can be cumbersome to the aircraft.

CHAPTER 6. WING DESIGN AND RECONFIGURATION DETAILS

Variable Sweep Wing

A variable-sweep wing or swing wing, is an airplane wing, or set of wings, that may be swept back and then returned to its original position during flight. It allows the aircraft's shape to be modified in flight, and is therefore an example of a variable-geometry aircraft.

While variable-sweep provides many advantages, particularly in reduction of drag, compactness of structure, load-carrying ability, and the fast, low-level penetration role, the configuration imposes a considerable penalty in weight and mechanical complexity. Also, the swing mechanism itself takes up too much space inside the wing. The box of the swing wing is also heavy to carry, slower to rise or turn.

Tensairity Structure Wing

The basic principle of tensairity is to use an inflatable structure to stabilize conventional compression and tension elements. It combines an airbeam with conventional cables and struts to improve the load bearing capacity of inflatable structures.

The weight of a tensairity structure is comparable to an optimized truss structure and much lighter than a simple inflatable structure for slenderness values typical in wings. Experimental tests confirm that the stiffness is much higher in tensairity compared to a corresponding conventional inflatable structure with the same internal pressure. The increased stiffness can be used to increase the span, for better performance or to increase the load bearing capacity of the wing. The lower pressure has consequences for the weight (use of lighter and cheaper materials) and the survivability. In case of a leakage it is much easier to compensate the air leakage with a small integrated pump, while still keeping structural rigidity. Since the rigid elements are placed inside the wing and thus protected by an air cushion, the tensairity wing has a good crash resistance.

Though tensairity structure solves almost all the issues related to inflated wing structure but tensairity wing can not be deployed by simple inflation due to the rigid compression elements. The set up requires some small assembly by inserting the compression elements in their pockets. Also, the ability to flex under gusts and overloads of a tensairity wing is slightly less compared to a normal inflatable wing due to the presence of the rigid compression elements[16].

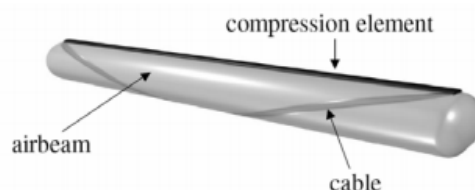


Figure 6.1: Basic Tensairity beam element

6.1.2 Selection Method: Weighted Matrix

For selection of final wing design, 15 wing design criteria were identified and defined. The list was evaluated and top 10 criteria were analyzed for various possible configurations. The configurations are rated out of 5 for each criterion.

CHAPTER 6. WING DESIGN AND RECONFIGURATION DETAILS

Table 6.1: Weighted decision matrix showing the various configurations ranked against the weighted criteria.

	Relative Importance (%)	Inflating	Folding & unfolding structure	Variable sweep	Tensairity
Compactness in hover configuration	15	5	3	1	3
Innovation	6	4	5	3	4
Load bearing capacity	25	2	4	4	3
Weight	20	5	3	2	3
Reliability	8	2	4	4	4
Mechanical complexity	8	5	2	2	3
Durability	4	2	4	4	3
Crash resistance/Safety	3	2	4	4	4
Ease of Deployment	7	5	5	4	1
Cost	4	4	3	3	4
Weighted Sum	5	3.7	2.46	2.9	3.07

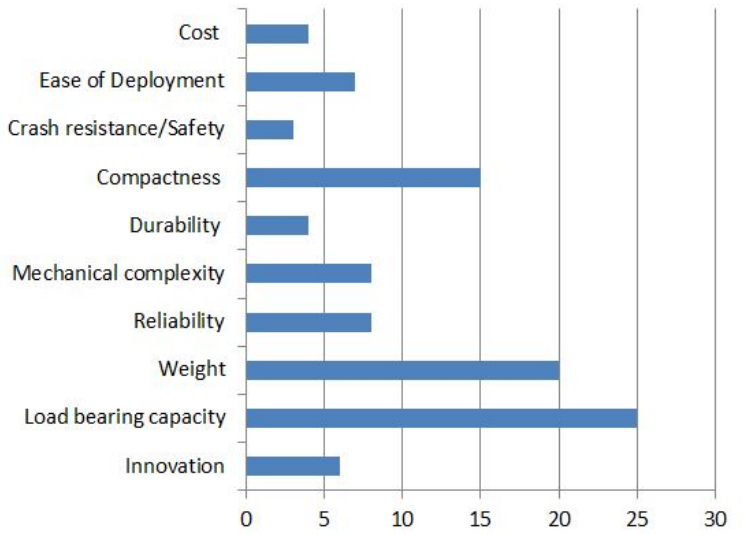


Figure 6.2: Relative Importance(%) of Wing Configuration Selection Criterion

6.2 Structural Design

Using the results of weighted decision matrix, it was considered that a configuration with combination of retracting internal structure with a covering of fabric maintained using low pressure would be most suitable for *Druta*.

Fully retracted wings in hover configuration produce a minimum download due to the air wash of rotors. During transition, the wings are designed to have a span of 7.5 m, thus gives larger lift and stall limit at lower speeds. Such a span also provides the gliding ability for the long range operations. The cruise flight takes place at the wing span of 6.5 m. The wing can be retracted back from fully extended configuration to support fast forward speed, and is helpful in achieving maximum dash speed.

6.2.1 Retracting Torque Box

The wing is mainly comprised of a single torque box, which is manufactured to run the length of the wingspan (6.5 m). Figure 3 shows the retracting torque box with the ribs and without the

CHAPTER 6. WING DESIGN AND RECONFIGURATION DETAILS

skin. The torque box was designed to provide the necessary stiffness to prevent the whirl flutter instabilities, as well as to support all of the anticipated aerodynamic and structural loads during normal flight operations. The torque box composed of front and rear vertical webs located at 12% and 52% of the chord, respectively.

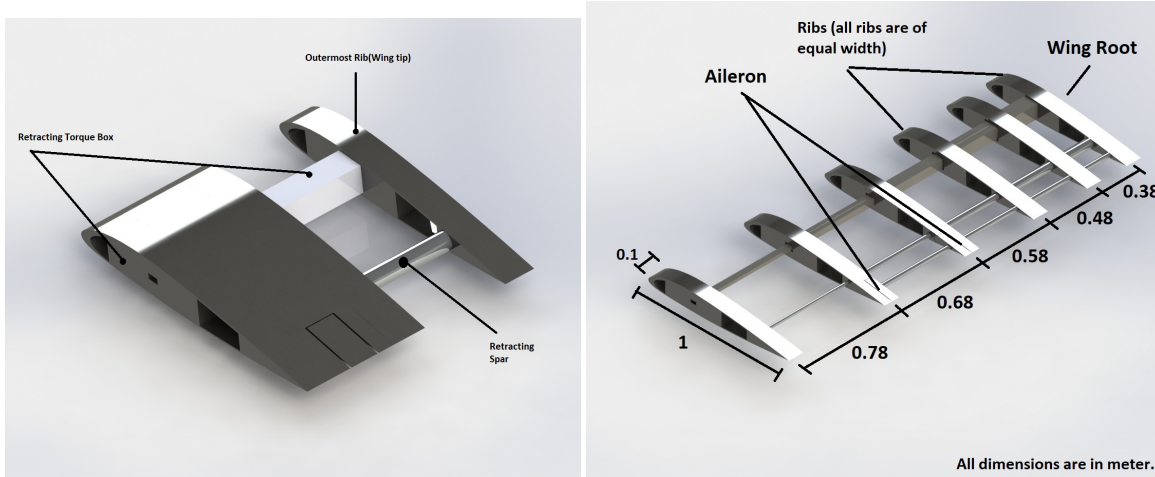


Figure 6.3: Retracting Torque Box in Expanded and retracted shape along with ribs and without skin.

6.2.2 Retracting Mechanism

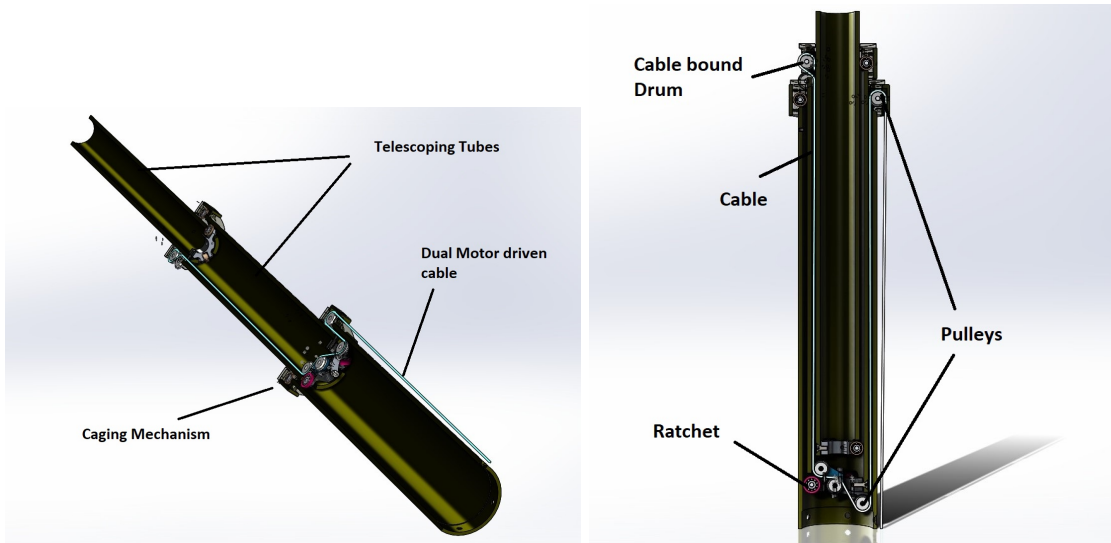


Figure 6.4: Sectional View describing the Retracting mechanism inside Torque box

A mechanical system is disclosed to deploy an antenna on a support which may, for example, be a spacecraft. A series of telescoping tubes are nested one within the other when the antenna is in a retracted stowed position. The outermost tube is rigidly attached to the support and the inner tubes are latched in the stowed position by a caging mechanism. The antenna is driven

CHAPTER 6. WING DESIGN AND RECONFIGURATION DETAILS

toward a deployed position by a dual motor driven cable which is terminated in a driving tube at the lower end of the innermost tube, from whence the cable is trained about pulleys at the tops and bottoms of successively large tubes of the antenna. The cable is wound on a drum at the lower end of the antenna and coaxial therewith. During deployment of the antenna, the drum rotates, thereby reeling in the deployment cable. The initial movement of the cable causes cam releasing of the latches in the caging device. Thereafter, the antenna tubes are extended until the final deployed position of the antenna is reached. A ratchet attached to the drum prevents reverse rotation of the drum and locks the antenna in the deployed position until the ratchet is released[17].

6.2.3 Initial Sizing

In conventional fixed-wing aircraft design, the structural components of the wing are sized to meet strength requirements based on the typical loads that are expected to act on the wing. The estimated wing loads are used to approximate the shear and moment distributions along the wing span. From the shear and moment distributions, the respective shear and bending stress acting along the wing is calculated and the torque box is sized to ensure a factor of safety of at least 1.5 for the most critical load case.

After initial sizing of the wing distributed loads and point forces were used to represent the aerodynamic forces, propeller thrust and wing weight at the MGTOW. An analysis of the wing was conducted based on Euler–Bernoulli beam theory and St. Venant torsion theory.

The maximum tip deflections and bending stresses were determined, and the torque box was resized to ensure that minimum rotor ground clearance and margins of safety under normal flight operations were fully met.

6.2.4 Inflation Mechanism

Wings are made up of fabric kind material so to prevent sagging of fabric between the ribs a pressure of 185-200 KPa is maintained inside the wing. To maintain this pressure turboshaft engine bleed air is used. The bleed air from compressor is carried to the wing. After reaching the required pressure the valve carrying the bleed air is closed. The bleed takes less than 50 seconds to completely fill the wings.

Previously using a nitrous oxide cylinder was also considered but it was decided otherwise because using the bleed air would eliminate need of using extra cylinder thereby reducing the weight. Also the wing can be inflated and deflated multiple times.

6.2.5 Material Selection

For Torque Box and Rib Structure

A graphite-epoxy composite material was chosen for the construction of the torque box and ribs because it met the high material stiffness requirements of the design while significantly reducing the empty weight of the aircraft. Table 1.2 shows the comparison of various materials considered for torque box and internal structure.

Table 6.2: Comparison of Various materials considered for Torque Box

Material	Density(kg/m ³)
Aluminium	2700
Graphite Epoxy	1600
Fibre Glass	1900

CHAPTER 6. WING DESIGN AND RECONFIGURATION DETAILS

The front and rear webs have a spacing of 0.40 m and a thickness of approximately 6 mm while the upper and lower sections of torquebox connecting the front and rear webs have a thickness of 8 mm. Because the wing is made of composite materials, it is able to be constructed as one long continuous unit from tip to tip.

For Skin Covering

Material chosen for the skin covering of Wing structure is VectranTM. VectranTM is a high-performance multifilament yarn spun from Liquid Crystal Polymer (LCP). It is the only commercially available melt-spun LCP fiber. VectranTM fiber exhibits exceptional strength and rigidity. Pound for pound, VectranTM fiber is five times stronger than Steel and ten times stronger than Aluminum.

VectranTM offers a distinct advantage over traditional metals in terms of strength-to-weight ratios as shown in Table 1.3 listing the tensile properties and densities of various reinforcing materials.

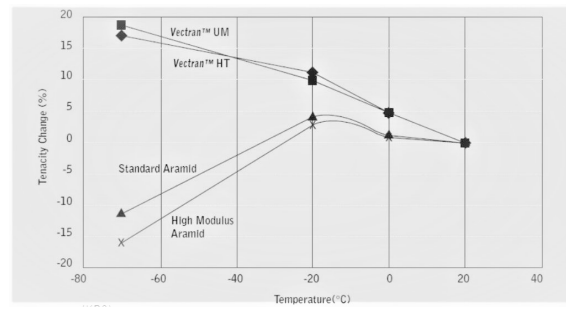


Figure 6.5: Low Temperature Properties of VectranTM Fiber

Table 6.3: Comparison of properties of various engineering materials for wing skin

Material	Density (gm/cm ³)	Tensile Strength (GPa)	Tensile Modulus (GPa)
Vectran TM NT	1.4	1.1	52
Vectran TM HT	1.41	3.2	110
Stainless Steel	7.9	2.0	210
Aluminum	2.8	0.6	70
E-Glass	2.6	3.4	72

Moreover, Low temperature performance of Vectran is much better than Aramid fibre which makes it usable at 3000 m.

The VectranTM is attached with the rib structure using Adhesives Master Bond EP21TDC-2LO. It is a two component, highly flexible epoxy resin compound for high performance bonding, sealing, coating, and encapsulation. It has a service temperature range of 4K to +250°F and has been successfully employed in a number of cryogenic applications. Master Bond EP21TDC-2LO is an exceptionally versatile system that offers the structural benefits of an epoxy, yet incorporates flexibility and very good thermal conductivity[18].

6.3 Reconfiguration Details

Druta is able to reconfigure on its own using components which remain onboard the aircraft at all times. The reconfiguration is reversible and can be executed multiple times without external support as and when required.

CHAPTER 6. WING DESIGN AND RECONFIGURATION DETAILS

To change the hover configuration to forward flight configuration, the wings are completely extended to the maximum span and two turbojet engines that are placed over the fuselage are started. When *Druta* gains a forward velocity sufficient to balance the downward force (around a stall speed of 30 m/s), rotor is stopped using the brakes and tilted to a horizontal position. Then, the rotor blades are retracted from a 1.5 m radius to a 1 m radius. Once the rotor tilting and retraction is complete, it is again started. As the thrust provided by the propeller reaches sufficient values to provide lift, the turbojets are turned off. Also, the inverted V-tail is extended. This completes the reconfiguration of the vehicle to forward flight. The rotor is stopped while tilting to prevent strong gyroscopic forces and increase the reliability of vehicle. Use of turbojets make the transition smooth and fast.

When it is required to change the vehicle from forward flight configuration to hover configuration, the turbojets are started and the rotor is stopped using the brakes. The blades are extended from a 1m radius to a 1.5 m radius and V-tail is retracted back. The rotor is tilted back by 90 degree to a vertical position and started again. The turbojets are stopped once the rotors produce enough lift. Thus the vehicle completes transition to the hover configuration. Finally the wings are retracted to have a maximum span of less than 3m in hover configuration. The system does not lose all of its forward momentum during this transition, the rotors with the swashplate mechanism can be used after the transition set to an appropriate speed.

Any minute control requirements during the lower speed phase (less than 20 m/s) of the transition is handled by the swashplate mechanism of the rotor while the 4 control surfaces handle control during the higher speed phases of the transition.

Wing extension and inflation using bleed air from compressor takes about 45 seconds to extend it to maximum span. Simultaneously the turbojets are started. *Druta* requires 50 seconds to reach the speed of 30 m/s with the thrust of the turbojets. The tilting rate of coaxial rotor is 10 degree/second. Rotor takes about 4 seconds to start again. So *Druta* takes about *105 seconds* in complete transition from hover configuration to forward flight.

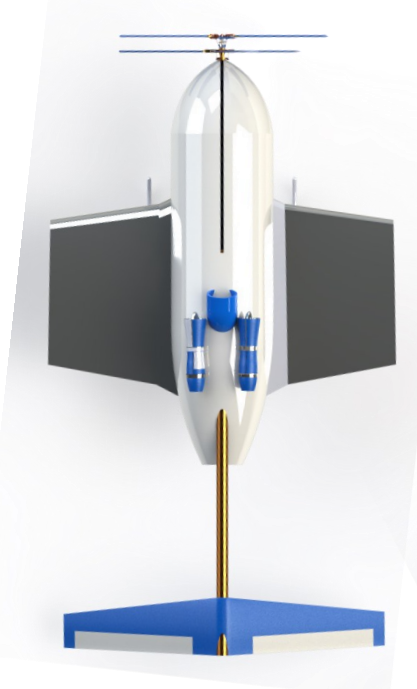
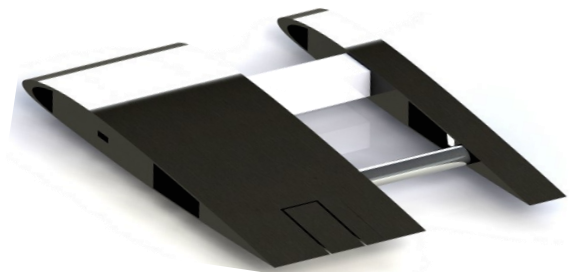
During reconfiguration from forward flight to hover, starting the turbojets require about 50 seconds. The turbojets are used to sustain thrust for lift while the rotor is made vertical. Titling occurs at the same rate of 10 degree/ second, along with extension of the rotor blades. After this, the rotor is started. Wing retraction and deflation occurs once the rotor is sped up to generate enough lift. Overall; the titling, extension and speeding up of the rotor takes 20 seconds. Retraction and deflation occurs very fast with air escaping within 8-10 seconds. through valves at the bottom of the wing. Thus, it takes about *80 seconds* in transition from forward flight to hover configuration.



Figure 6.6: Reconfiguration procedure

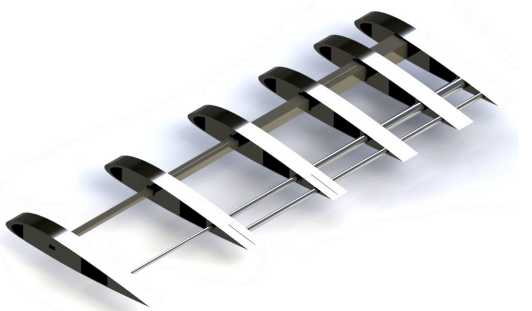
Span-wise adaptive wings

Hover



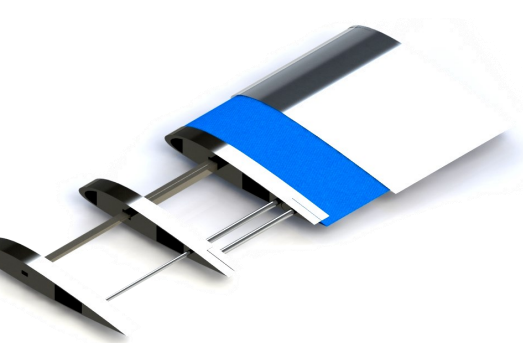
The fully retracted wings produce a minimum download in hover configuration due to the air wash of rotors. This decreases the power requirement during hover and increases the hover time.

Transition



During transition, wing span opens up to the tip to tip length of 7.5 m, thus reaching the required thrust value at minimum. Such a span also provides the gliding ability for the long range operations.

Cruise



The cruise flight takes place at the wing span of 6.5 m. The wing can be retracted back from fully extended configuration to support very fast forward speed, and is helpful in achieving maximum dash speed.

Wingspan of Druta is varied using a retracting torque box and skin covering of Vectran. Wings are retracted in hover configuration while completely extended to a span of 6.5m in forward flight configuration.

The wing is mainly comprised of a single torque box, which is manufactured to run the length of the wing-span. The torque box provides the necessary stiffness to prevent the whirl flutter instabilities, as well as to support all of the anticipated aerodynamic and structural loads during normal flight operations. A graphite-epoxy composite material is used for the construction of the torque box and ribs as it meets the high material stiffness requirements of the design while reducing the weight at the same time. Skin covering of wing structure is made up of Vectran. Vectran is a high-performance multifilament yarn spun from liquid crystal polymer (LCP). It is the only commercially available melt-spun LCP fiber. Vectran fiber exhibits exceptional strength and rigidity. Pound for pound, Vectran™ fiber is five times stronger than Steel and ten times stronger than Aluminum. Wings are made up of fabric kind material so to prevent sagging of fabric between the ribs a pressure of 185-200 kPa is maintained inside the wing. To maintain this pressure the engine bleed air is used. The bleed takes less than 50 seconds to completely fill the wings.



DRUTA

7. Drive Train

7.1 Engine Selection

Many engines are eliminated due to weight constraints and desired performance parameters. Engines like electric, turbojet, turboshaft, and reciprocating/piston diesel engine were considered. Trade studies were performed to determine the best engine for *Druta*[19, 20, 21]. The design trades considered were performance, development time, cost, maintainability, size and weight.

Table 7.1: Comparison of various engine configurations considered

Type of Engine/Engine configuration	Advantages	Reason for rejection
Hovering using turbojet/turbofan and forward flight using deflected slipstream.	No tilting of rotor required. Design is simple and elegant.	For attaining the required thrust for hover, weight of engine is very high. Also the specific fuel consumption is very high.
Turboshaft for hovering and only Turbojet for forward flight.	No tilting required.	Dead weight of Turboshaft engine and the rotor during forward flight. Also the specific fuel consumption for jet is very high.
Hybrid engine along with tiltrotor.	Higher efficiency, Easier control over power and RPM of rotor.	The power to weight ratio of IC engine was quite high, also the weight constraint does not allow the weight of motor, generator and battery
Only Turboshaft for both forward flight and hover.	Higher power to weight ratio	Difficult to control during transition.
Turboshaft engine for hover and both turboshaft and turbojet for forward flight.	Easier to control during transition. The jets aren't very heavy and also facilitate higher maximum speed. Plus all the advantages of turboshafts.	-

A turboshaft engine was selected for *Druta* as it has high power-to-weight ratio, more time-between-overhaul requirements and requires less frequent servicing in comparison to piston engine. Turboshaft engines also have the advantage that they are able to start at lower ambient temperatures and can provide full power without a long warm-up period, which makes them ideal in this case.

The Rotax 914 was initially considered but rejected due to the weight. The final decision had to be made between RR 300/500 vs Rolls Royce M250(Allison Model 250)[22, 23]. According to the final analysis M250 C10B[24] was found to be better for our requirements. The weight of the engine is 74 Kg delivering the maximum take-off power of 298 KW and max continuous power of about 287 KW.

It was decided to use two turbojets TJ23U by PBS[25] each having the weight of 2 kg and could provide the thrust(max) of 230 N. This can also help reach a higher maximum speed than by only the propeller. During the cruise the turbojet engines are switched off.

Table 7.2: Selected properties of Rolls Royce M-250 C10B

Engine Property	Value
Max Take-off Power	236 KW
Max Continuous Power	201 KW
Output Shaft RPM	6000
Engine Weight	63 Kg
Specific Fuel Consumption (Approximately)	0.47-0.51 kg/KW.h
Dimensions (Length x Width x Height)	1035*480*585

Table 7.3: Properties of the turbojet TJ23U by PBS (Each Engine)

Engine Property	Value
Weight	2 Kg
Thrust (Max)	230 N
Specific Fuel Consumption	0.65 l/min
Dimensions (Diameter x Length) (mm)	121 x 316

The decision of engine was done on the basis of the power required and the transmission efficiency which is 85%.

7.2 Transmission Design

The aim of this section is to design and model a transmission system that would take input from the turboshaft engine and distribute power to the two contra-rotating rotors. Both the upper and lower rotors are designed to operate at same rotational speeds throughout the mission but having different direction of rotations. Vehicle speed and size are critical parameters for *Druta*. Because of the need of maximizing range and speed, the major consideration while designing the transmission system was to minimize gearbox weight while maximizing efficiency, compactness and strength. The others parameters that were considered in design process of the transmission system are overall simplicity, ease of assembly/ disassembly, vibration minimization and manufacturability issues[26].

Tilting of output shaft occurs through a tilting mechanism without any reduction ratio change after tilting[27].

7.2.1 System Configuration

The M250 C10B turboshaft drives the system with an input of 6000 rpm which gets reduced 1500 rpm both in hover and during forward flight through transmission System. Rotor Assembly is tilted during transition from hover to forward flight or vice-versa. Reduction ratio is 4 in hover and forward flight.

This reduction in the RPM was achieved by single stage planetary gear. Figure 9.1 shows the layout and gives relevant information about the engine and the transmission system. Such an configuration is chosen to increase compactness.

So in the final design of transmission system, engine is mounted below the coaxial rotor system hub lying on the line passing through length of fuselage. Since the reduction ratio is same in both hover and forward flight, no coupling or decoupling of gears is required during transition which makes transmission very reliable. Output shaft is tilted by 90 degree during transition.

Table 7.4: Transmission gear specifications.

Stage	Satellite/Sun	Satellite/Crown
No. of teeth (pinion/gear)	24/8	24/32
Reduction ratio	3	1.33
RPM (pinion/gear)	6000/2000	2000/1500
Module	2	2

Nickel chromium steel alloy are considered as material for the transmission system due to its high hardness and good wear resistance. And also nickel chromium alloys are economical. The total weight of the transmission system is estimated to be 32 kg.

Hydraulic brakes have been used to as it allows for better control accuracy. Hydraulic systems are simple, safe and economical because they use fewer moving parts compared to mechanical and

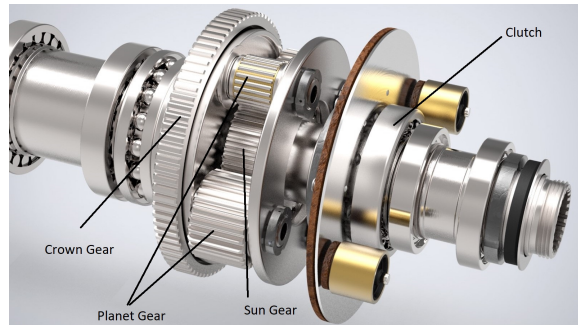


Figure 7.1: Planetary Gearbox with clutch plate and brakes

electrical systems, which makes them easier to maintain.

7.2.2 Gearbox Casing

The gearbox casing is to be manufactured from aluminum through die casting because of its large size. Although magnesium is about 30% lighter than aluminum, it has a much lower strength and is susceptible to corrosion especially in saltwater environments. Magnesium also has a higher thermal expansion rating, which would affect the overall alignment of the transmission as it is heated or cooled. After each gearbox casing is finished, it should be laser scanned and compared to the CAD model to ensure the required tolerances are met. A cone shaped mast housing alleviates the lift from the rotors being placed directly on the gearbox casing and transmission; the connection points transfer the lift to the torque box in the wing.



Figure 7.2: Gearbox casing

8. Performance Analysis

8.1 Drag Estimation

Parasitic drag on the body during forward flight was estimated using the “Equivalent Skin-Friction Method”[28]. It is based on the fact that the system in subsonic cruise will have parasite drag that is mostly skin-friction drag plus a small separation pressure drag. The equivalent skin friction coefficient was taken as 0.0065. This value was chosen as *Druta* is similar to a propeller seaplane (similarities being the propulsion method and skid landing gears. The ratio of wetted area to reference area is 2.00394[14]. Thus the parasitic drag coefficient is equal to the product of equivalent skin friction coefficient and the ratio between wetted and reference area. After increasing the value by 20% to account for extra drag due to the engine air intakes and landing legs, the value of the first order drag polar was found to be 0.0159. The second order drag polar was found using from the Oswald span efficiency method[14]. Using the empirical formula given for a straight wing the Oswald span efficiency factor was 0.854. With this value and an wing aspect ratio of 6.5, the “drag due to lift” coefficient was found to be 0.0573. Thus, the following table gives the important speeds for different operational altitudes. Note, drag at cruise is constant at all altitudes.

Table 8.1: Cruise speed for different operational altitudes

Height	SLS	At 1500m	At 3000m
Cruise Speed (m/s)	53.5	57.2	61.8

8.2 Vehicle Download

The combined thrust produced by the rotors in hover must exceed the total weight of the vehicle because of the download created by the rotor wake as it impinges on the wing and the fuselage. A download penalty always requires higher power requirements in hover and low speed flight. For the *Druta*, the download is alleviated by the retraction of inflated wings and use of an inverted V-tail, so that the wings and tail play a minimal role in downwash generation. Furthermore, the fuselage has been made aerodynamic from forward flight as well as hover point of view. A downwash penalty of 4% of the gross weight has been observed at hover. This makes an addition of 240N to the existing weight of the VTOL.

8.3 Hover Performance

The hover design point for the vehicle is at 3000 m, -4.49°C at MGTOW as well as at SLS. The available power in Hover Outside of Ground Effect (HOGE) conditions is greater than that required. At the HOGE design point, the required power at 3000m altitude is 167 kW and 156 kW at SLS excluding the transmission efficiency of 85%. With a fuel capacity of 133 kg, the following values has been calculated for the VTOL to hover:

CHAPTER 8. PERFORMANCE ANALYSIS

Table 8.2: Hover time values for 50% and 100% fuel usage

	Fuel Usage	Hover Time
At altitude of 3000 m	50%	72 minutes
	100%	138 minutes
At SLS	50%	78 minutes
	100%	149 minutes

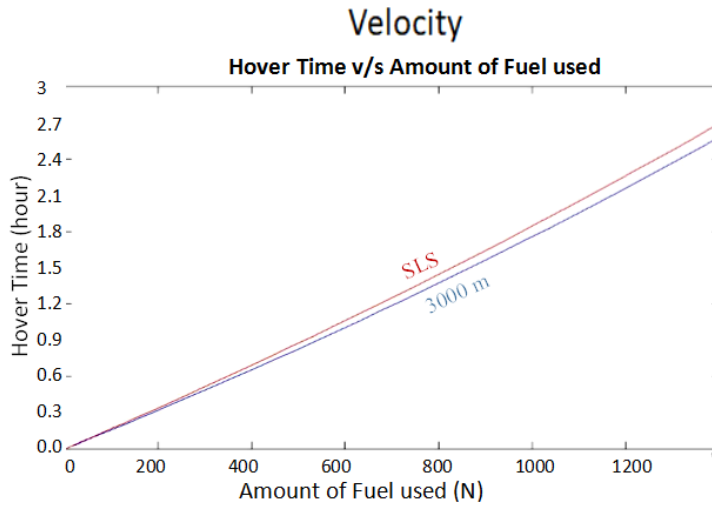


Figure 8.1: Variation of hover time with the amount of fuel used

8.4 Dash Speed

The dash speed of an airplane is set by the maximum thrust it can reliably sustain until all fuel reserves run out. In the design of *Druta*, the use of jet engines for the reconfiguration was not the only purpose. The twin jet engines, while not used for cruise flight, can be switched on for providing additional thrust to the main propeller thrust. The jet engines account for a roughly constant thrust output over multiple operating altitudes. The thrust from the jet engines account for 32-35% of the total maximum thrust. The main difference in dash speed at different operating altitudes is due to the difference in thrust produced by the propeller. The following table summarizes the dash speed at different altitudes[28].

Table 8.3: Maximum speed values at different operational altitudes

Height	Maximum thrust available (N)	Dash speed (m/s)
SLS	1273.4	141.8
At 1500m	1166.7	144.8
At 3000m	1060.0	148.7

Thus, the estimated drag area of the system at different altitudes are
The formula used to calculate the drag area was

$$\text{Drag Area} = \frac{\text{Drag Force}}{\frac{1}{2}\rho V_{max}^2} \quad (8.1)$$

CHAPTER 8. PERFORMANCE ANALYSIS

Table 8.4: Equivalent drag area for different operational altitudes

Height	Drag area (in sq m)
SLS	0.1055
At 3000m	0.1065

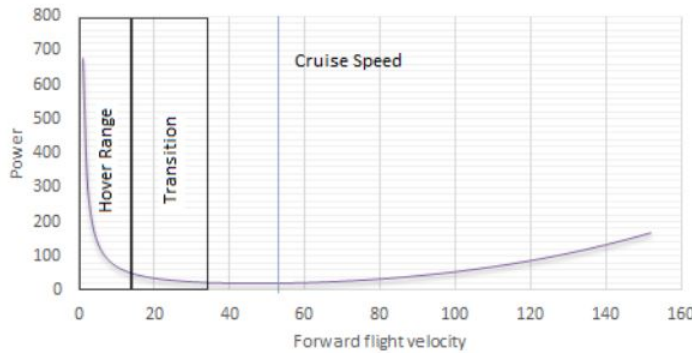


Figure 8.2: Variation of power required with velocity

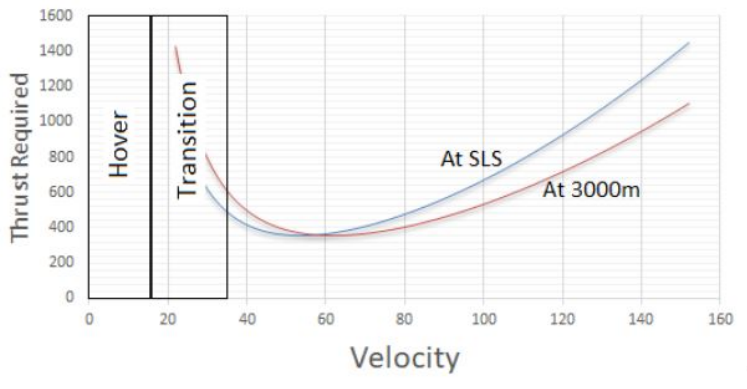


Figure 8.3: Variation of thrust required with velocity

8.5 Range

The range of a plane was calculated at a speed where the lift to drag ratio was minimum. It is assumed that in cruise only the propeller is used for maximum efficiency. The range was calculated using the Breguet range equation. It is assumed that the specific fuel consumption and lift to drag ratio would more or less remain constant during operation[28]. The range of the system for different operational altitudes at 50% energy consumed is tabulated below.

Table 8.5: Maximum range values for different operational altitudes

Height	Range (km)
SLS	431.17
At 3000 m	497.88

8.6 Autorotational Capability

To compare the potential auto rotational capabilities of *Druta* to other helicopters and tiltrotors, an estimate of the Autorotative Index (AI) was made. The AI depends on the stored kinetic energy of the entire rotor system (i.e., on the blade mass, radius of gyration, and its angular velocity) and the vehicle gross weight. Because *Druta* employs relatively high tip speeds in the hover mode, the stored inertia in the rotor is also relatively high. The larger stored inertia coupled with the increased radius and low disk loading in hover allows *Druta* to achieve an AI equivalent to multi-engine helicopters of similar MGTOW, as shown in Figure. The ability to auto rotate as good as a helicopter, glide to a landing in airplane mode, and successfully perform all of the missions under single-engine-out conditions gives *Druta* an unprecedented level of performance and safety of flight compared to any type of rotary-wing vehicle that is currently flying.

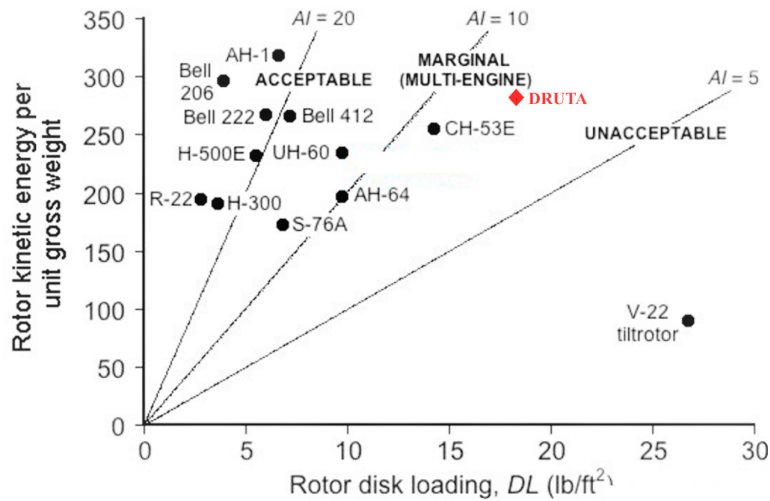


Figure 8.4: Comparison of autorotative index for different rotorcraft

9. Landing Gears

There is the need for the vehicle to reconfigure on the ground for its easy movement on the ground inside the hanger. For this reason the rotor would have to be tilted and thus would make the landing gear analysis complex. Since the vehicle is capable of taking off without fully reconfiguring(using the turbojets), it was decided that the landing gear would not be made according to the rotor tilting since the size of rotor calls for a very long landing gear which means more complexity and unnecessary weight.

9.1 Landing Gear Types Considered

Due to weight constraints forward flight is not considered as part of design of Druta. Therefore fixed skids were chosen[29].

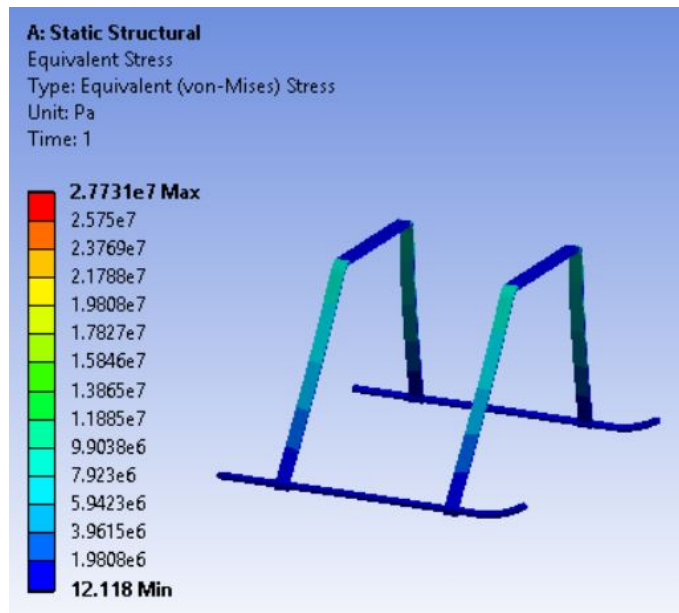


Figure 9.1: Gearbox casing

The inverted V tail is 0.6 m lower than fuselage so in compliance with the FAR 25 provision requires a landing gear of 0.7 meters.

The landing gear configuration was selected on the basis of criteria required by FAR[30, 31].

A static stress analysis was performed on the landing gear using ANSYS Static Structural. The material for the landing gear used for the analysis was Aluminum 1060 H-18 alloy. A geometrical fixture was applied on the upper rods and a force little more half of the gross take-off weight of the *Druta* was applied to both the lower skid rods. The maximum stress found was less than yield stress of the material, so no failure occurred.

9.2 Static Stability Angle Analysis

The position of the ground contact points in relation to the center of gravity of the aircraft (helicopter) defines the pitch and roll static stability angles. To ensure static lateral stability of the helicopter, the roll stability angle must be less than 60° . Similarly, static pitch stability is guaranteed when the pitch angles is less than 30° . *Druta*'s landing gear was designed to ensure pitch and roll stability. The roll/tip over angle is 57.99° , and the pitch angle is 16.26° .

10. Airframe Structure

The structural layout of *Druta*'s fuselage consists of three sections mainly

- Payload and fuel section
- Transmission and engine section
- Tail section

Rotor is mounted at the CG in the hover configuration and comes forward in forward flight configuration. There is a slot in fuselage to allow this transition. The airframe was designed to maximum space for the payload while maintaining a low drag shape. Additional design considerations included preparedness for harsh environments and to create a highly reconfigurable aircraft for multi-mission operations. Since wings do not carry any load other than their own weight, this increases the structural efficiency of wing to fuselage connection points.

10.1 Structural Details

The fuselage of *Druta* consists of four primary bulkheads and one secondary bulkhead. The secondary bulkhead is to support the rotor in forward flight configuration. The first primary bulkhead supports the payload. The second and third primary bulkhead is for supporting the transmission, wing and rotor in hover configuration. The fourth primary bulkhead supports the main engine and V-tail. Two jet engines placed over the fuselage are supported by the third and fourth primary bulkheads together. There are also many thin stringers that were included in the airframe in order to reduce the load on bulkheads and maintain the shape of the skin. The cross-section of the fuselage is circular in shape. There is a slot in front two primary bulkheads to facilitate tilting of main rotor. [32]

Druta is designed as a low winder plane. For the vehicle to be used as a surveillance plane, a low wing provides better visibility at the sides of an aircraft. Low wing configuration also causes better ground effect which increases lift and reduces drag of the aircraft when it is nearer to the earth's surface and it supports the landing gears.

The total fuel for the mission is kept in two cylindrical fuel tanks to avoid the CG shift. These fuel tanks are kept near the bottom corners of the fuselage.

10.2 Material Selection

Aluminum-Lithium (Al-Li) was chosen for the construction of the main fuselage because it is lighter than standard aluminum and can be manufactured using traditional techniques. The bulkheads, stringers and keel beams of the airframe are made up of composites. The airframe skin and rotor hubs were also of the composites. The engine deck is made of titanium alloy plate with honeycomb structure for its high resistance to heat and fire, as well as oil corrosion. Aluminum alloys were considered for the skid landing gear of *Druta*.

The tail is a composite construction to reduce weight. In addition to reducing weight, the composite structure is resistant to many of the harsh environments in which the aircraft will likely be operating.



11. Weight and CG Analysis

All coordinates of the CG analysis table are in the plane parallel to the Right Hand Side View (RHSV). The x-axis is along the longitudinal dimension of the fuselage while the z-axis is along the vertical. The entire system is symmetric in the third dimension. The origin of the coordinate system is placed on the lower left corner of the fuselage as seen in the RHSV.

The shift in CG observed during transition dictated the placement of the components. The rotor axis lies above the CG in the hover configuration, with a maximum deviation of 5 cm from CG at MGTOW. During forward flight; the center of thrust, center of lift and CG are nearly collinear. Variation in payload and fuel amounts cause the CG to shift upto 6 cm from CG at MGTOW.

Table 11.1: Weight and CG Analysis details of *Druta*

Name of Part	Hover		Forward Flight		Weight (kg)	Weight% (Gross weight)	Weight% (Empty weight)
	X _{cg} (m)	Z _{cg} (m)	X _{cg} (m)	Z _{cg} (m)			
Rotor Group	0.98	0.97	0.33	0.26	45.48	12.41	7.58
Tail section	2.1	0.37	2.8	0.37	12	3.28	2
Wing Group	0.85	0.26	0.85	0.26	30.66	8.37	5.11
Fuselage Group	0.98	0.4	0.98	0.4	39.72	10.84	6.62
Landing gear group	0.95	-0.36	0.95	-0.36	12.9	3.52	2.15
Nacelle group	1.6	0.9	1.6	0.9	18	4.91	3
Propulsion group	1.55	0.3	1.55	0.3	70	19.10	11.7
Fuel system	1	0.25	1	0.25	19.8	5.40	3.3
Drive system group	0.98	0.28	0.98	0.26	32.52	8.88	5.4
Flights control group	0.8	0.25	0.8	0.25	36.8	10.04	6.1
Auxiliary power group	0.5	0.2	0.5	0.2	4.62	1.26	0.8
Instrument group	0.1	0.1	0.1	0.1	7.32	2.00	1.2
Hydraulics group	0.95	0.18	0.95	0.18	13.32	3.64	2.2
Electrical group	0.8	0.3	0.8	0.3	7.5	2.05	1.3
Avionics group	0.1	0.05	0.1	0.05	6.88	1.88	1.1
Furnishing and equipment	1	0.4	1	0.4	8.88	2.42	1.5
Payload(OutBound)	0.5	0.3	0.5	0.3	100		16.67
Fuel	1	0.17	1	0.17	133.6		22.3
	0.967	0.319	0.932	0.264	600	100	100



12. Avionics and Control systems

12.1 Requirements

The main challenges of the mission are long travel distances, high altitude flying, intermediate speed limit of jet and propeller propelled planes, reconfiguration of vtol, and a variety of ground obstacles including powerlines. The mission is divided into two key phases with unique sensor requirements

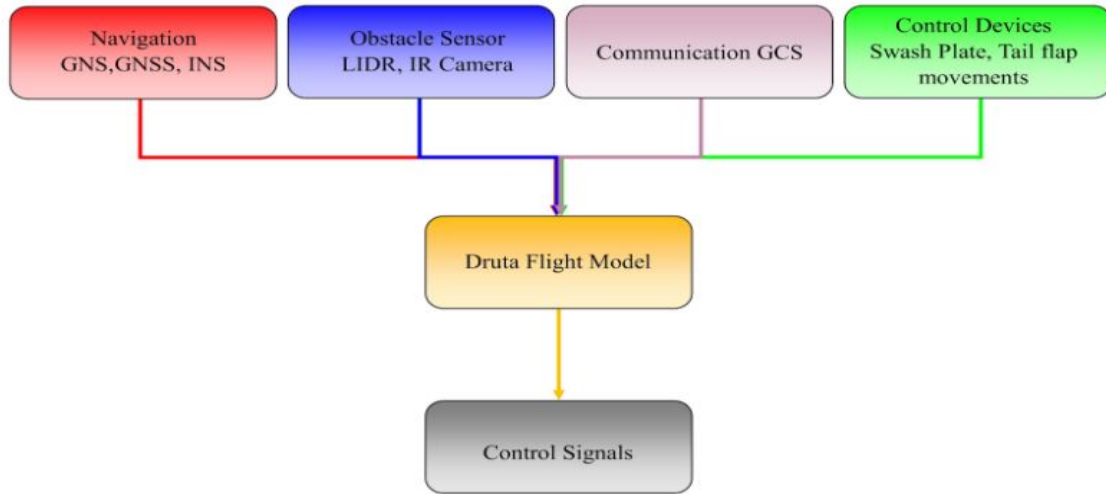


Figure 12.1: General flow diagram of signal flow

12.1.1 Avionics and Sensors

Auto-pilot: This system is responsible for guiding motion in fixed wing and hovering configuration. The autopilot unit consist of a microcontroller and multiple sensors; on the bases of which control signals are given to actuators. The unit should also be capable of processing data from different sensors and give accurate signals during the reconfiguration of the vehicle. UAV autopilot -VECTOR is capable of controlling both fixed and rotor based flying systems. VECTOR contain inbuilt GPS and INS with sufficient degrees of freedom (3 from accelerometer , 3 from magnetometer ,3 of gyroscope, 1 form temperature , 1 from pressure sensor). For safety, it contain redundant sensors and power connections. The unit is compact with dimensions of 45.0 x 68.0 x 74.5(mm), weight of 180 g and draws power of 2.5 W[33]

Inertial Navigation System (INS):It provides the direction of motion without the need of any reference frame and is critical for carrying out the accurate transition between the two modes of flight. For accurate aircraft motion, the Air Data Aircraft Heading and Reference System (ADAHRS) needs to provide accelerometer reading in three direction, gyroscopes reading of three direction, a magnetometer, a pressure sensor reading and reading from temperature sensor.

CHAPTER 12. AVIONICS AND CONTROL SYSTEMS

Satellite Navigation: To deliver the payload at given location precisely navigation instruments should be able to provide accurate data regarding aircraft's location. Global Positioning System (GPS) receivers typically has a 3.0 m location accuracy. If the plane were to carry its own transmitter and receiver, power consumption and weight will increase significantly. Instead, using a number of satellite groups, accuracy (upto 2 cm) and reliability can be increased. Trimble BD920 GNSS Receiver is integrated in the VTOL avionics system to enable access to GPS, GLONASS, Galileo, QZSS and SBAS satellite constellations and provide horizontal location accuracy of 2.0 cm and vertical location accuracy of 4.0 cm. This receiver also provides horizontal velocity with an accuracy of 0.024 km/hr and vertical velocity with accuracy of 0.072 km/hr[34].This receiver will be used with Novatel 42GOXX16A4-XT-1-1-CERT antenna.

Obstacle Sensing and Avoidance: In missions involving hovering near ground, obstacle sensing and avoidance is critical. Light detection and ranging create a three dimensional point cloud, which will be used to define a path and motion for the VTOL. Velodyne PUCK Lite LIDAR is capable of generating 3D map of surfaces using 300,000 points per second, in a range of 100m and 3cm accuracy on a 30 degree with vertical FOV and 360 degree horizontal FOV. The VTOL scans the surface beneath using LDIR in hover mode to find suitable site for landing or for the delivery of the payload.

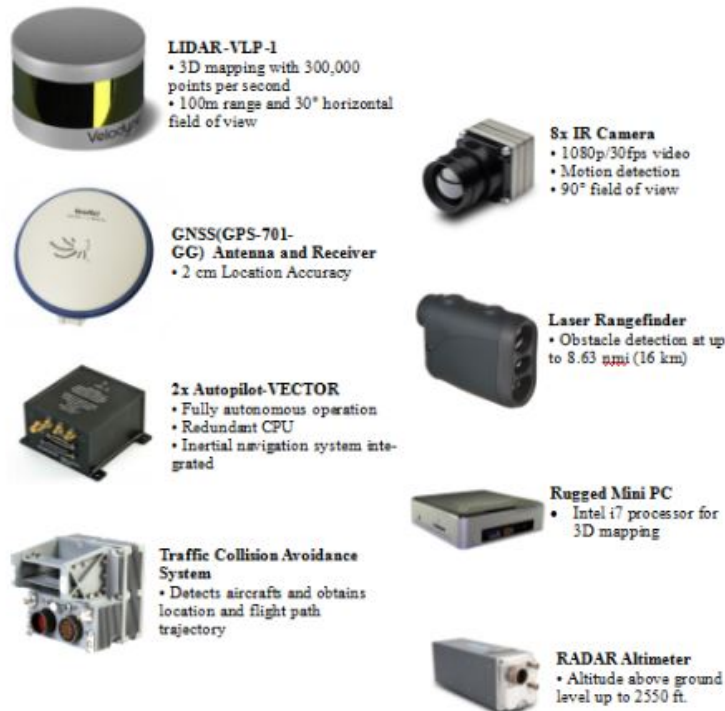


Figure 12.2: Avionics components

CHAPTER 12. AVIONICS AND CONTROL SYSTEMS

Table 12.1: Avionics system components

Component	Quantity	Power(W)	Wight(kg)
CPU(zini-1660)	1	40	0.45
LiDAR Sensor - VLP-1	1	8	0.83
Battery	3	89wh	0.468
IR (FLAIR Quark2)	8	1	0.05
GNSS(Trimble BD920)	2	1.3	0.024
GNS antenna(GPS-701-GG)	2	1.2	0.5
TCAS BAE system	1	40	2.7
Radar altimeter	1	13.75	1.59
Radar altimeter antenna	2	-	0.27

12.2 Sensor Operation

12.2.1 Control system initialization

During mission initialization, basic mission plan are loaded into the system with the help of an interactive user interface unit (touch screen). This includes destination location and all the landing sites, in case of emergency. By running sensor check test (software) system will check for errors and if no errors are found sensors will be turned on. Another important system which is needed to start the system is a power plant. As *Druta* is a jet powered aircraft and jet engines are not self starting in nature ,so external system (other than jet engine) is needed. This can be done using external high pressure air to have perfect air fuel mixture or another way is to rotate the engine shaft using an external electric motor. In *Druta* we are using TJ23U(2kg) by PBS and M250 C10B (63kg) , both are light weight engines hence electric motor starting is preferred. So onboard electric motor will run M250 C10B which will further help in starting TJ23U. With sensor initialization and engine start, phase one is complete and phase two begins, sensors will measure airspeed around the *Druta* and set coaxial rotor to cancel airspeed effect. According to the mission requirement *Druta* will either stay in hover mode or prepare it for forward flight transition by extending the wings are starting the jets.

12.2.2 Vertical Flight and Hover

LIDAR Based SLAM: In hover mode *Druta* will remain close to the ground, moving in a low speed range. In these situations LIDAR and INS will generate a 3D map which will help guiding through the terrain. This will further help in finding a suitable location from where *Druta* can reconfigure from hovering mode to forward flight mode. This complex task will be done by assigning scores based on parameters which include distance from *Druta* (based on GPS coordinates), deviation from pre-planned location, comparison of characteristics of location to other locations. The location with highest score will be the selected for reconfiguration. A similar procedure will be followed to find a landing site.

12.3 Flight Control System

General Control signal flow diagram of *Druta* is shown in Figure 12.1. The altitude and latitude controller was designed based on the flight models of a coaxial helicopter and a plane with an

inverted V tail; in which transition requires stopping of rotor and using it tilting it into a propeller while using a jet engine in the intermediate process to generate the required thrust for lift. V in the flow diagram represents state-space of flight $V = [u, v, w, p, q, r, \dots]$. The controller features primarily a linear-quadratic regulator (LQR) based feedback, which regulates swashplate movements of both the rotors during all other stages of the mission. While the LQR control scheme requires knowledge of all the states of the system, it is appropriate as the control system because of its performance and robustness.

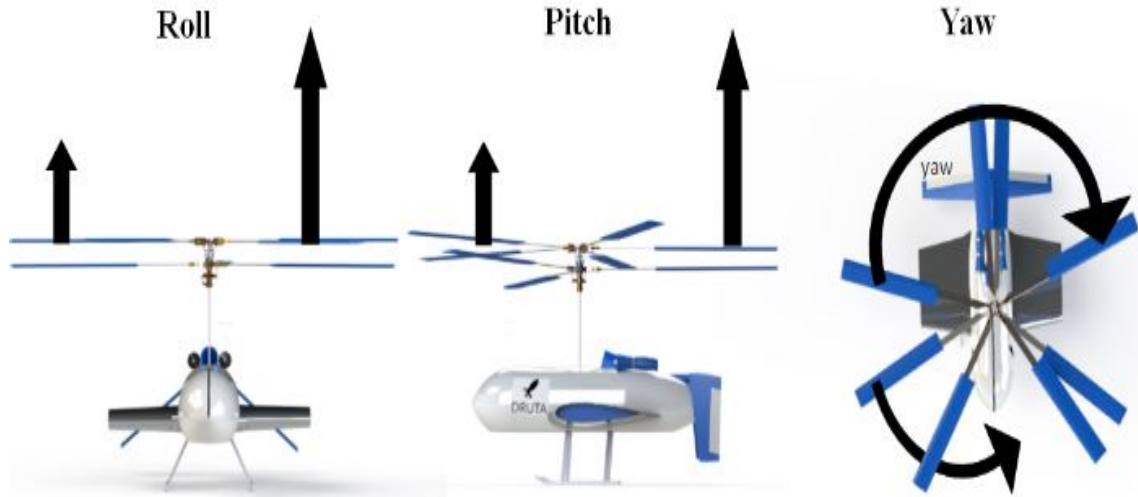


Figure 12.3: Roll, Pitch and Yaw control in hover configuration

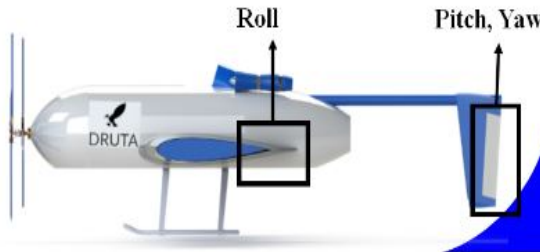


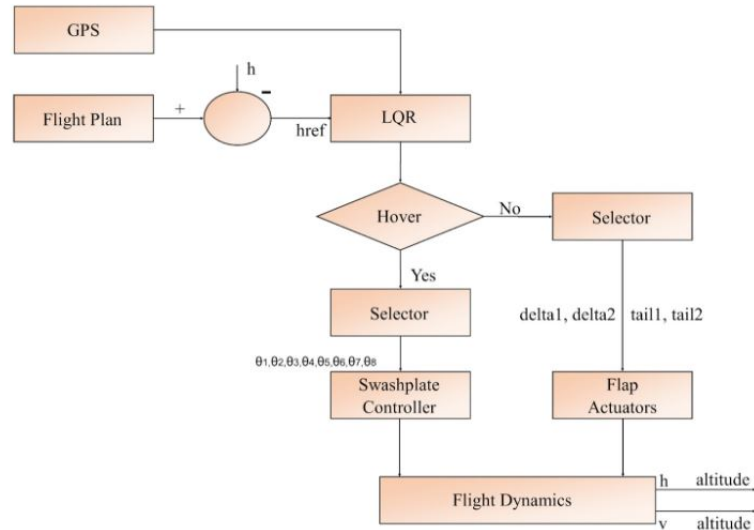
Figure 12.4: Roll, Pitch and Yaw control during cruise

12.3.1 Yaw control

In hover mode, yaw can be controlled by applying different torque on coaxial rotors, so increasing the torque on the rotor rotating clockwise direction will result in rotation in the anticlockwise sense. By increasing pitch angle of clockwise rotating rotor and decreasing pitch angle of second rotor, drag will change on both rotors and hence the torque required. This system needs two swashplates for controlling both rotors[35] this method is being used in Ka-50 Black Shark. In forward flight inverted v tail flaps need to be controlled to get yaw moment.

12.3.2 Pitch and roll control

Pitch and roll can be controlled by collective and cyclic pitch to rotors. The accomplishment of the collective and cyclic control for the coaxial configuration is very much like that of the single main rotor helicopter. The two swashplates are given the same input signal. So for both collective and cyclic control, the two rotors will behave as one.



$\{\theta_1, \theta_2, \theta_3, \theta_4, \theta_5, \theta_6, \theta_7, \theta_8$ refer to pitch angle of individual rotor blade.
 δ_1, δ_2 , represents deflection in ailerons while tail1,tail2 represents angles of two parts of V-tail.}

Figure 12.5: Design of Control systems for *Druta*

13. Cost Analysis

13.1 Acquisition Cost

The cost of tiltrotor as with other aircraft is divided into various categories: development cost, production cost, and operational costs. These categories add up to the total life-cycle cost of the vehicle.

For the analysis, the estimation of the cost is based on historical data. All costs are presented in U.S. dollars. An empirical model developed by *Harris and Scully* has been used for estimating the tiltrotor cost. This model uses historical trends. This empirical model proves to be effective at estimating helicopter cost but has yet to be proven for tiltrotors. However, being the most readily available and widely accepted method for estimating cost, this model would be used to estimate the cost of *Druta*. The formula is as follows:

$$Price = \$236.77(H)(Blades\ Per\ Rotor)^{0.2045}(Wgt.\ Empty)^{0.4854}[Eng(s).\ Rated\ HP]^{0.5843} \quad (13.1)$$

where H is a product and is computed using

$$H = Engine\ type \times No.\ of\ Engines \times No.\ of\ rotors \times Landing\ gear \times Pressurization \quad (13.2)$$

Table 13.1: H factor vs Aircraft properties

		Value	Engine Type	Value	Country	Value
Engine Type	Piston	1.000	Single	1.000	US commercial	1.000
	Piston(converted to turbine)	1.180	Multi	1.352	US military	0.838
	Turbine	1.779	-	-	Russia	0.330
Main Rotor Type	Single	1.000	Fixed	1.000	Yes	1.135
	Twin	1.046	Retractable	1.104	No	1.000

Taking into account the inflation per year in the US, the factor was modified in order to calculate the cost for the current aircraft; the cost of *Druta* is estimated to be about *1.135 million* US dollars[36, 37].



14. Summary

BITS Pilani undergraduate team has designed *Druta*, a variable diameter coaxial tiltrotor with spanwise adaptive wings, to meet all of the vehicle and operational requirements for the Aero India 2019. It is a unique innovative design and has an edge over an other existing VTOL aircrafts.

The conclusions of *Druta's* design are as follows:

- Innovative spanwise adaptive wings provide compactness in hover configuration and reduce the downwash area. Inflating wing with internal structure reduces weight and vibrations too.
- Advanced variable diameter coaxial tiltrotor provides required thrust in hover configuration with lower disk loading and in forward flight configuration with lower tip speed.
- Novel combination of 5 blades and 3 blades in the coaxial rotor system is acoustically preferred design. It reduces noise when used in a city type environment.
- Use of two jet engines along with main turboshaft engine give higher maximum velocity and faster transition from hover to forward flight.



Figure 14.1: *Druta* in both hover and forward flight configuration over a mega city

Bibliography

- [1] URL: <https://vertipedia.vtol.org/vstol/wheel.htm>.
- [2] T.L Saaty. *Multi-criteria Decision Making: The Analytic Hierarchy Process*. 1990.
- [3] Inderjit Chopra Marat N. Tishchenko Vengalattore T. Nagaraj. *Preliminary Design of Transport Helicopters*.
- [4] Wayne Johnson. *NDARC — NASA Design and Analysis of Rotorcraft Theoretical Basis and Architecture*.
- [5] Washington D.C.: U.S. Federal Aviation Administration. U.S. Government Printing Office. *DISC LOADING—The total helicopter weight divided by the rotor disc area*.
- [6] Demo J. Giulianetti Maisel Martin D. and Daniel C. Dugan. *The History of the XV-15 Tilt Rotor Research Aircraft: From Concept to Flight*.
- [7] URL: https://dspace-erf.nlr.nl/xmlui/bitstream/handle/20.500.11881/503/53%5C_8.PDF?sequence=1.
- [8] P. C. K. Robert E. Sheldahl. *Aerodynamic Characteristics of Seven Symmetrical Airfoil Sections Through 180-degree Angle of Attack for Use in Aerodynamic Analysis of Vertical Axis Wind Turbines*.
- [9] URL: https://www.researchgate.net/publication/233591485_Hover_Performance_Correlation_for_Full-Scale_and_Model-Scale_Coaxial_Rotors.
- [10] URL: <http://nptel.ac.in/courses/101106041/20#>.
- [11] URL: https://www.faa.gov/regulations_policies/handbooks_manuals/aviation/helicopter_flying_handbook/media/hfh_ch04.pdf.
- [12] URL: <http://www.aerospaceweb.org/question/airfoils/q0041.shtml>.
- [13] John D. Anderson. *Fundamentals of aerodynamics*. 2001.
- [14] Daniel P. Raymer. *Aircraft design: a conceptual approach*. 1989.
- [15] Suzanne Smith Jamey D. Jacob Andrew Simpson. *Design and Flight Testing of Inflatable Wings with Wing Warping*. 2005.
- [16] Rolf H. Luchsinger Joep Breuer Wubbo Ockels. *An inflatable wing using the principle of Tensairity*.
- [17] W. A Leavy and C. R. [Inventor] Griffin. *Antenna deployment mechanism for use with a spacecraft. [extensible and retractable telescopic antenna mast]*.
- [18] INC. KURARAY AMERICA. *Vectran Liquid Crystal Technology*.
- [19] Sikorsky “Full-size helicopter runs on 100% electric power”. URL: <http://www.dvice.com/archives/2010/07/sikorsky.php>.
- [20] Sikorsky “Project Firefly: Sikorsky Unveils Electric Helicopter Technology demonstrator”. URL: <http://www.gizmag.com/sikorsky-project-firefly/15993>.
- [21] GIGA, “Lithium Ion Battery - 45 Ah, 3.6 V”. URL: http://www.gaia-akku.com/fileadmin/user_upload/downloads/en/Handling_HP602030NCA-45Ah.162Wh.pdf,%202009..
- [22] URL: [http://rg1.faa.gov/Regulatory_and_Guidance_Library/rgMakeModel.nsf/0/54c499656ba5570b862575b4004d8d65/%5C\\$FILE/E4CE.pdf](http://rg1.faa.gov/Regulatory_and_Guidance_Library/rgMakeModel.nsf/0/54c499656ba5570b862575b4004d8d65/%5C$FILE/E4CE.pdf).

BIBLIOGRAPHY

- [23] URL: <https://www.verticalmag.com/features/thelittleenginethatdid>.
- [24] URL: <https://www.rolls-royce.com/products-and-services/civil-aerospace/helicopters/m250-turboshaft.aspx>.
- [25] URL: <http://www.pbsaerospace.com/our-products/tj-20-turbojet-engine>.
- [26] D. W. Dudley. *Handbook of Practical Gear Design*. 2002.
- [27] URL: <https://vtol.org/files/dmfile/excalibur1.pdf>.
- [28] John D. Anderson. *Aircraft performance and design*. 1999.
- [29] Louis. Hrusch. *Articulated Main Landing Gear*. 1976.
- [30] URL: <https://www.law.cornell.edu/cfr/text/14/25.925>.
- [31] URL: http://www.dept.aoe.vt.edu/~mason/Mason_f/M96SC08.pdf.
- [32] URL: https://www.faa.gov/regulations_policies/handbooks_manuals/aircraft/amt_airframe_handbook/media/ama_ch01.pdf.
- [33] URL: <https://www.uavnavigation.com/products/autopilots/vector>.
- [34] URL: http://www.trimble.com/OEM_ReceiverHelp/v5.11/en/BD920%5C%20PDF.pdf.
- [35] URL: <http://www.aerospaceweb.org/question/helicopters/q0034.shtml>.
- [36] URL: <http://www.inflation.eu/inflation-rates/united-states/historic-inflation/cpi-inflation-united-states.aspx>.
- [37] URL: http://ae.metu.edu.tr/~ilkay/Dr.Ilkay_Yavrucuk_Homepage/Misc_files/Rotorcraf%5C%20Cost%5C%20too%5C%20much.pdf.